# Chapter 3
# Chitin and Chitosan Based Blends, Composites and Nanocomposites

**Mohammad Zuber, Khalid Mahmood Zia and Mehdi Barikani**

**Abstract** Nature is gifted with several nanomaterials which could be obtained from different animal and plant sources. Cellulose, chitin and starch are abundant, natural, renewable and biodegradable polymers. By intelligent processing techniques they could be used as classical nano reinforcing fillers in polymers i.e., composites. They are often called whiskers.

## 3.1 Introduction

Nature is gifted with several nanomaterials which could be obtained from different animal and plant sources. Cellulose, chitin and starch are abundant, natural, renewable and biodegradable polymers. By intelligent processing techniques they could be used as classical nano reinforcing fillers in polymers i.e., composites. They are often called whiskers. These whiskers are almost defect free and as a result, their properties are comparable to perfect crystals. The excellent reinforcing properties of these natural whiskers stem from their chemical nature and hierarchical structure. During the past decade, many studies have been devoted to mimic biocomposites by blending natural whiskers from waste and biomass sources with various polymer matrices. The presence of crystalline fibrils in the chitinous integuments has been elucidated several decades ago [1–3]. This chapter intends to

M. Zuber (✉) · K. M. Zia
Department of Applied Chemistry, Government College University, Faisalabad 38000, Pakistan
e-mail: mohammadzuber@gmail.com

M. Barikani
Department of Polyurethane, Iran Polymer and Petrochemical Institute, Tehran, Iran

S. Thomas et al. (eds.), *Advances in Natural Polymers*,
Advanced Structured Materials 18, DOI: 10.1007/978-3-642-20940-6_3,

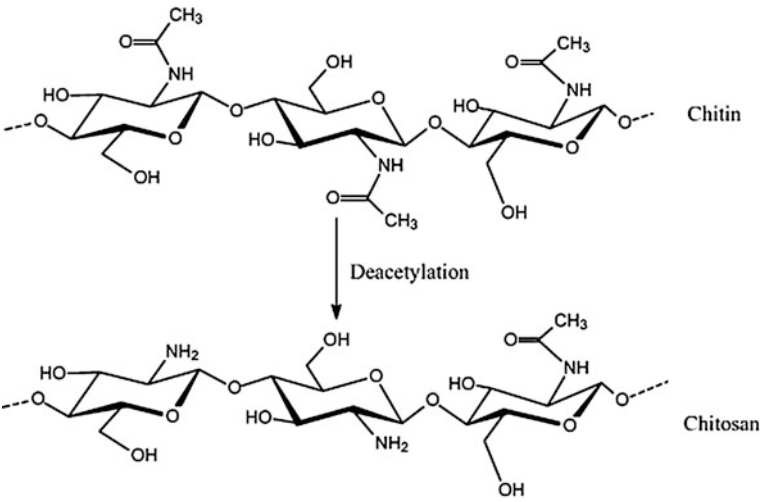


**Fig. 3.1** Chemical structure of chitin and deacetylated chitin (chitosan)

focus on the chitin and chitosan based blends, composites and nanocomposites. During the last few years, however, some indications appeared in the literature about the preparation of composites made of chitin whiskers dispersed into natural and artificial polymers. It is believed that this subject represents at this time an opportunity for a better exploitation of chitin, as well as a challenge in view of certain technical difficulties.

Chitin is a naturally occurring polysaccharide and is recognized by consisting of 2-acetamido-2-deoxy- D-glucose via a $\beta$ (1–4) linkage (Fig. 3.1). As the second most abundant biopolymer after cellulose, chitin occurs in enormous number of living organisms such as shrimps, crabs, tortoise, and insects, [4] and can also be synthesized by a nonbiosynthetic pathway through chitinase-catalyzed polymerization of a chitobiose oxazoline derivative [5–7]. Chitosan, as the most important derivative of chitin, can be prepared by its chemical modification. Chitin and chitosan have many excellent properties including biocompatibility, biodegradability, non-toxicity, absorption properties, etc., and thus they can be widely used in variety of areas such as biomedical applications, agriculture, water treatment and cosmetics. In addition, there is a reactive amino group on the structured units of chitosan (Fig. 3.1). The amino group makes chitosan much easier to be modified by chemical reactions than cellulose. A lot of derivatives of chitosan with different functional properties have been synthesized by chemical modifications. There are many reviews focusing on the properties, modifications and applications of chitin and chitosan [8–10]. This chapter focuses on the other aspects of chitin: chitin nanoparticles and their applications especially in reinforcing polymer nanocomposites. Polymer nanocomposites refer to multiphase materials consisting of a polymer matrix and nanofillers. They show distinctive properties even at minimum loading of nanofillers, due to the nanometric size effect, in comparison

with virgin polymer and conventional polymer composites [11]. Following the successful development of nylon-clay nanocomposites in 1985 [12], the polymer nanocomposites have attracted a great deal of interest from both academic and commercial point of view due to their appealing unique properties [13, 14]. Conventionally used nanofillers are inorganic compounds especially layered nanoclays, such as montmorillonite (MMT) and layered double hydroxides (LDH), with homogeneous dispersion in polymer matrix [15]. Renewable semi-crystalline polysaccharides like cellulose, chitin and starch consisting of crystalline domains and amorphous domains are possible candidates for organic nanofillers, since the amorphous domains can be removed under certain conditions such as acidolysis and the crystalline domains with high modulus can be isolated in nano-scale. Then the nano-sized crystalline particles, usually known as polysaccharide nanocrystals, can be used as reinforcing nanofillers in polymer nanocomposites. Since Favier et al. [16] reported the use of cellulose nanocrystals as reinforcing nanofillers in poly(styrene-co-butyl acrylate) (poly(S-co-BuA))-based nanocomposites in 1995, the polysaccharide nanocrystals have drawn a large interest in polymer nanocomposites due to their excellent intrinsic properties such as nano-sized dimensions, high surface area, biodegradability, non-toxicity, renewability, low density and easy modification conferred by the large amount of surface hydroxyl groups [17–20]. Some recent reviews have been reported on preparation, properties, modifications and applications of cellulose, starch and chitin nanocrystals [15, 17, 21–25].

## 3.2 Structure of Chitin

The structure of chitin is very analogous to cellulose (Fig. 3.2). They both are supporting materials for living bodies i.e., for both plants and animals, with sizes increasing from simple molecules and highly crystalline fibrils at the nanometer level to composites at the micron level upward [26]. Thus, they intrinsically have

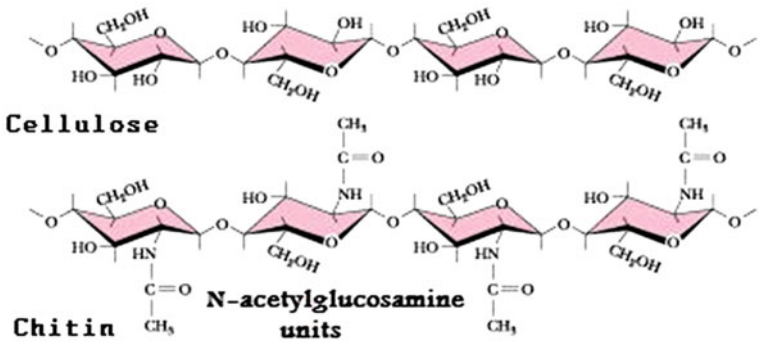


**Fig. 3.2** Chemical structure of cellulose and chitin

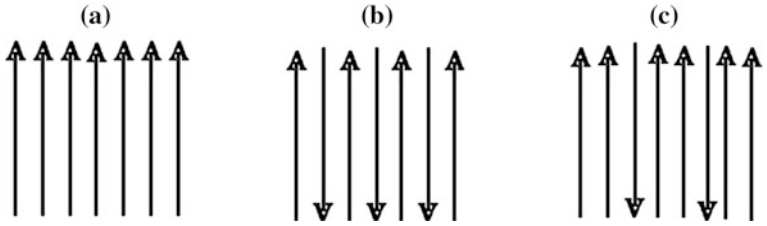


**Fig. 3.3** Three polymorphic configuration of chitin **a** α–Chitin, **b** β–Chitin, **c** γ-Chitin

the potential to be converted to crystalline nanoparticles and nanofibers and to find applications in nanocomposite fields. Chitin whisker can be prepared from chitin isolated from chitin containing living organisms by the similar method towards preparation of cellulose whiskers through hydrolysis in aqueous solution of strong acids.

Marchessault et al. [27] for the first time reported a route for preparing suspension of chitin crystallite particles in 1959. In this method, purified chitin was first treated with 2.5 N hydrochloric acid solution under reflux for 1 h, the excess acid was decanted and then distilled water was added to obtain the suspension. They found that acid-hydrolyzed chitin spontaneously dispersed into rodlike particles that could be concentrated to a liquid crystalline phase and self-assemble to a cholesteric liquid crystalline phase above a certain concentration [28, 29]. The chitins are polysaccharides and are present within numerous taxonomic groups. However, on commercial scales chitins are usually isolated from marine crustaceans, mainly because a large amount of waste is available as a by-product of food processing. In this case, α-chitin is produced while squid pens are used to produce β-chitin. The structure of α-chitin has been investigated more extensively than that of either the β- or γ- form, because it is the most common polymorphic form. Very few studies have been carried out on γ- chitin. It has been suggested that γ- chitin may be a distorted version of either α- or β-chitin rather than a true third polymorphic form [30]. In α–chitin, the chains are arranged in sheets or stacks, the chains attaining the same direction or 'sense'. In α- chitin, adjacent sheets along the *c* axis have the same direction; the sheets are parallel, while in β-chitin adjacent sheets along the *c* axis have the opposite direction, as antiparallel arrangement. In γ- chitin, every third sheet has the opposite direction to the two preceding sheets [30]. A schematic representation of the three structures is shown in Fig. 3.3.

The underlying chitin matrix in the crab shell and its microfibrillar structure is shown in Fig. 3.4. This chitin is termed as α-chitin because of its crystal structure. Treatment of this chitin with 20 % NaOH for 1–3 h at 120 °C gives a 70 % deacetylated chitin (chitosan), which is soluble in many dilute acids. The detailed method is given in Sect. 3.4. The repetition of this step can give deacetylation

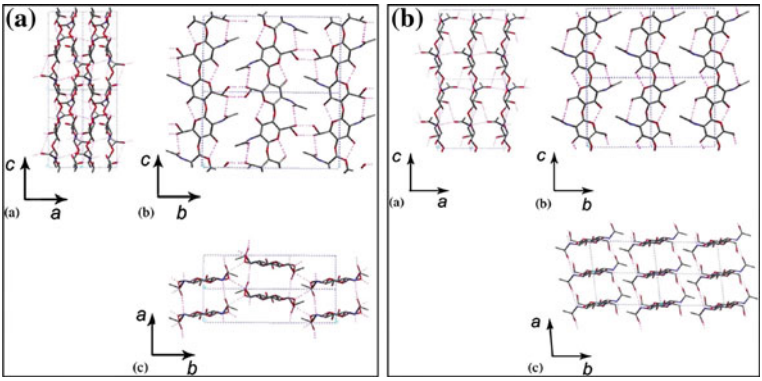


**Fig. 3.4** Structures of α-chitin (**a**) and β-chitin (**b**) [215]

values up to 98 %. A more reactive form of chitin is obtained from squid pens [28, 29]. This β-chitin is easily isolated and has a looser chain packing in the crystal, accounting for its higher reactivity and solubility in formic acid. The isolation of β-chitin is accomplished by first washing the squid pens in 1 M HCl for 12 h, followed by a 12 h treatment with 2 *M* NaOH. The final step is to heat the pens at 100 °C for 4 h in fresh 2 *M* NaOH. This procedure yields 35 % chitin from the mass of the pens. The degree of acetylation may be up to 92 %.

It is worth mentioning that crustaceans protect themselves from predators and pathogens by secreting an acellular exoskeleton including calcite crystals within the fibrillar organic network. The organic matrix is made of four superimposed layers (Fig. 3.5a). The epicuticle (ep) and pigmented (pi) layers are deposited before moult; the principal (pr) and membranous (mb) layers are deposited after moult. The matrix, composed of chitin associated with proteins, is produced by an underlying monolayer of epidermal cells (Fig. 3.5b). In a lower ratio, the cells also secrete lipids mostly in the epicuticle and pigments in the pigmented layer. The enzymes, for example alkaline phosphatase and carbonic anhydrase, are also synthesized in relation with the control of calcification, which occurs in the two middle layers (pi and pr) [31]. Carbonic anhydrase producing carbonate ions shows maximum activity during the first stages of calcification just after the moult. The enzyme enhances the precipitation of calcium carbonate; it was shown that diamox, its inhibitor, depresses the growth rate of calcite crystals in the cuticle. In domains where the section plane is transverse to the fibril axis, a honeycomb pattern reveals the elementary chitin protein units (high resolution TEM). Ultrathin section of the principal layer of the chitin-protein fibrils are seen in longitudinal, oblique or transverse view forming well defined strands (Fig. 3.5c). The clear central rods, a few nanometres in diameter, correspond to chitin crystallites; the dark sheath corresponds to the binding proteins (Fig. 3.5d).

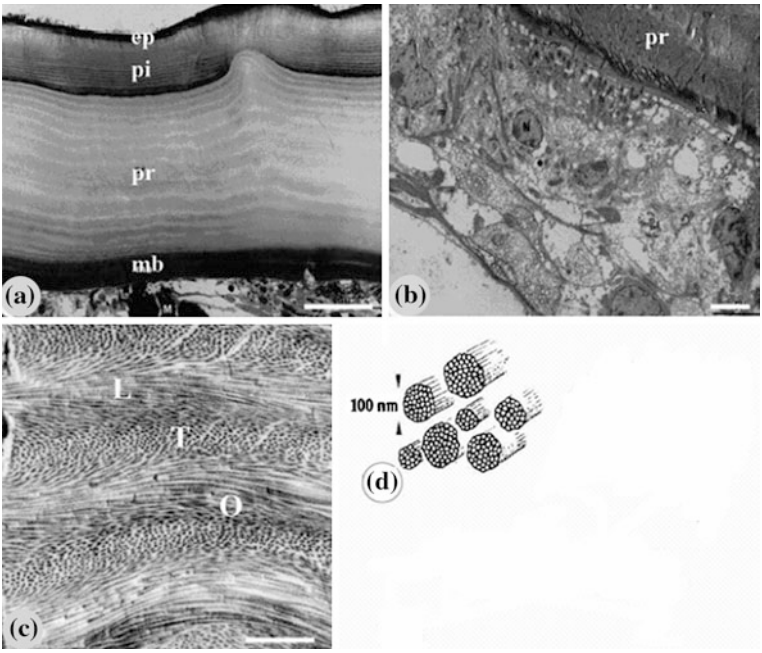


**Fig. 3.5** The chitin-protein matrix of the crab cuticle. **a** Semi-thin section normal to the carapace, from top to bottom: epicuticle (*ep*), pigmented layer (*pi*), principal layer (*pr*), membranous layer (*mb*). Optical microscopy, bar = 50 μm. **b** Ultrathin section of the principal layer of the cuticle and the underlying epidermal cells. TEM, bar = 5 μm. **c** Ultrathin section of the principal layer, the chitin-protein fibrils are seen in longitudinal, oblique or transverse view forming well defined strands. TEM, bar = 1 μm. **d** Aspect of the chitin protein fibrils observed at high magnification in TEM; the central electron light chitin crystals are surrounded by a sheath of contrasted proteins [31]

## 3.3 Properties of Chitin Whiskers

Similar with preparation of cellulose nanocrystals, the main process for isolation of chitin nanocrystals is also based on acid hydrolysis [32]. Disordered and low lateral ordered regions of chitin are preferentially hydrolyzed and dissolved in the acid solution, whereas water-insoluble, highly crystalline residues that have a higher resistance to acid attack remain intact. Thus, following an acid hydrolysis that removes disordered and low lateral ordered crystalline defects, chitin rodlike whiskers are produced [16, 17]. Unlike tunicin whiskers which can only be prepared by hydrolysis in strong sulfuric acid ($H_2SO_4$) solutions [16, 33], chitin whiskers (CWs) can be prepared by hydrolysis in hydrochloric acid (HCl) solutions. Revol et al. [34] and Li et al. [35] reported an approach towards preparation of suspension of chitin crystallites through acid hydrolysis in detail. In this approach, the purified chitin was hydrolyzed by boiling solution of 3 N HCl for

**Table 3.1** Sizes of chitin whiskers prepared from different origins

| Chitin origin | Hydrolytic time (hr) | Chitin whisker size | | References |
|---|---|---|---|---|
| | | Length | Width (nm) | |
| Squid pen | 1.5 | 150 | 10 | [36] |
| Riftia tube | 1.5 | 2200 | 18 | [37] |
| | 1.5 | 240 | 15 | [39] |
| | 1.5 | 500 | 50 | [38] |
| | 6 | 255 | 31 | [53] |
| Shrimp shell | 1.5 | 417 | 33 | [41, 42] |
| | 1.5 | 200–500 | 10–15 | [43] |
| | 3 | 200–560 | 18–40 | [55] |
| | 6 | 427 | 43 | [202] |
| | 6 | 549 | 31 | [217] |
| | 6 | 343 | 46 | [44] |

90 min; after acid hydrolysis, the suspensions were diluted with deionized water followed by centrifugation and Decantation of the supernatant; this process was repeated several times until the suspension spontaneously transformed into a colloidal state. The obtained crystallites were rodlike particles with average size of 200 ± 20 nm in length and 8 ± 1 nm in thickness. Because of the nanoscale size, the acicular crystal shaped can be called as nanocrystals or whiskers. Based on these procedures, whiskers have recently been prepared from many chitins of different origins such as squid pen chitin, [36] riftia tubes [37], crab shells [38–40], and shrimp shells [41–44]. The detailed information for CWs prepared from different origins of chitins is summarized in Table 3.1. The obtained rodlike whiskers showed similar size in width and were all in range of 10–50 nm irrespective of their origins and hydrolytic time. However, the lengths of the whiskers vary a lot in the range of 150–2200 nm for different origins of chitin, which may be ascribed to the different original sizes of the chitin particles and the diffusion controlled nature of the acid hydrolysis. The typical morphologies and sizes (average length and width) of dilute CW suspension observed by TEM and AFM are given in Figs. 3.6a and 3.6b [38, 39]. The suspension contains chitin fragments consisting of both individual microcrystals and associated or collapsed microcrystals. The length and width of the rodlike CW can be measured from the micrographs (Table 3.1) depending on the chitin origins. The principle towards preparation of polysaccharide nanocrystals is on the basis of the different hydrolytic kinetics between amorphous and crystalline domains [17]. That is to say, both the amorphous and the crystalline phases of polysaccharides can be hydrolyzed during treatment with aqueous solutions of strong acid. The swelling and hydrolysis of amorphous phases occur much faster than those of crystalline phases due to the regular tight arrangement of molecular chains in the crystalline domains. It is well established, documented and known that the boiling hydrochloric acid can easily dissolve the amorphous domains of chitin [45]; however, it can also break the ether and amide linkages of chitin [46]. So after removal of the amorphous domains,

the surface of crystallites will be attacked by the excess acid thus undergo further hydrolysis. Then controlling hydrolytic extent of chitin is very important for the preparation of CW with desired size and good yield. Except for the original sizes of chitin, concentrations of HCl and hydrolysis time are the two important factors for controlling the particle sizes and yield of chitin nanocrystals. The optimal concentration is 2.5–3 N which was widely used in preparation of CWs from chitin of different origins [32–34, 36–44]. The crystals of chitin are destroyed significantly with increase of HCl concentration, and they are completely dissolved in 8.5 N or higher HCl solutions [32, 46]. When 3 N HCl was applied, the hydrolytic time does not significantly affect the size especially cross-sectional width of the nanocrystals, since the whiskers showed similar lateral diameters in range of 10–50 nm within different hydrolysis times between 1.5 and 6 h, regardless of the original chitin sources. Recently, TEMPO-mediated oxidation (2,2,6,6-tetramethylpiperidine-1-oxyl radical mediated oxidation) method, which succeeded in preparing cellulose nanocrystals [47] and nanofibers [48–50], has also been successfully applied in the preparation of chitin nanocrystals [51] and nanofibers [52]. Almost individualized chitin nanocrystals with width less than 10 nm can be prepared from both $\alpha$-chitin and $\beta$-chitin with this method based on two steps, i.e., oxidation followed by ultrasonic treatment.

TEMPO-mediated oxidation of chitin occurred in water at pH 10 in the presence of NaBr and NaClO. During oxidation, chitin was converted into water-soluble polyuronic acid and water-insoluble particles, and the ratio of contents of both parts can be controlled by the amount of NaClO in the system. The water-soluble polyuronic acid products should be produced by oxidation of disordered domains or outer space of ordered domains of chitin, and the water-insoluble particles were the crystallites of chitin. Some hydroxyl groups of water-insoluble particle surfaces were converted to carboxyl or carboxylated groups during oxidation. When the carboxylated group containing crystallites were subjected to ultrasonic treatment, mostly individualized chitin nanocrystals were obtained, and the aggregation was hampered by existence of carboxylate groups on surface of the nanocrystals. In comparison with the conventional method, TEMPO-mediated oxidation method has many advantages: TEMPO-mediated oxidation is more controllable by the amount of NaClO and the yield of water-insoluble particles can reach 90 %; individualized nanocrystals with narrow width (less than 10 nm) can be obtained; besides, no N-deacetylation of chitin occurs during TEMPO-mediated oxidation. Figure 3.6c shows the TEM image and sizes of the obtained whiskers. In comparison with Fig. 3.6a (conventional CW), much more individual whiskers are formed by TEMPO method although some associated crystals could also be observed.

More recently, individual chitin nano-whiskers have been prepared from partially deacetylated $\alpha$-chitin by fibril surface cationization. When CWs with degrees of N-acetylation (DNAc) 0.74–0.70 were mechanically disintegrated in water at pH 3–4, individualized nano-whiskers with average width and length of $6.2 \pm 1.1$ and $250 \pm 140$ nm respectively, were successfully prepared, as reported by Fan et al. [52] the driving force for individualization of CWs is the same as that in

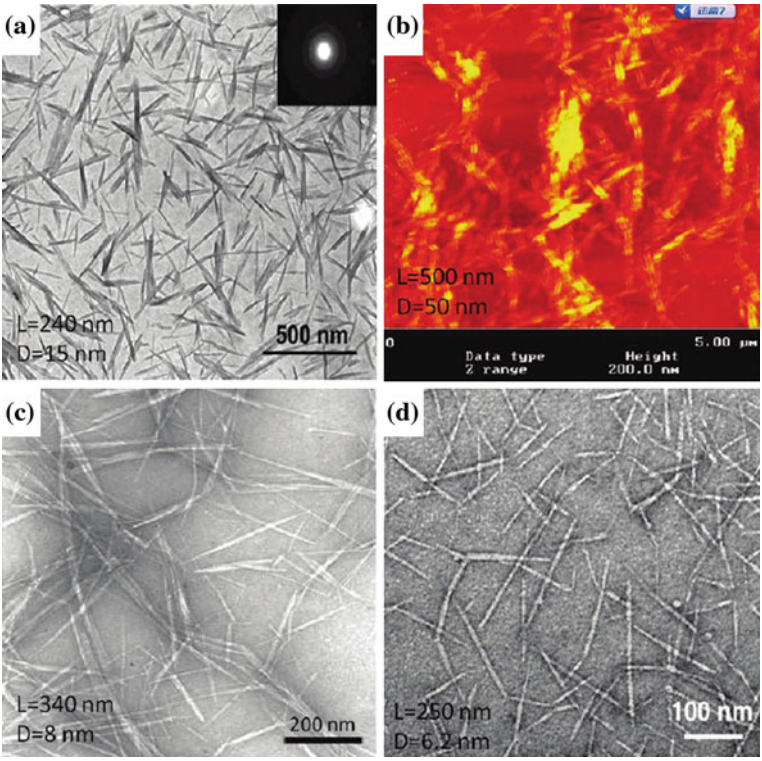


**Fig. 3.6** TEM (**a**) [39] and AFM (**b**) [38] images of a dilute suspension of chitin whiskers and TEM images of individual chitin whiskers obtained by TEMPO method (**c**) [51] and surface cationization (**d**) [53]

TEMPO-mediated oxidation method, i.e., surface charge induced electrical repulsion. The difference in the two methods are that TEMPO mediated oxidation endows CW surfaces with anionic charges while cationic charges for the latter. The TEM photograph and size of the individual CW are shown in Fig. 3.6d, some long individual fibrils, with widths similar to those of the whiskers but lengths of more than 500 nm were observed, which have not been reported in previous CWs prepared by the conventional method. The properties of nano-dispersions and casting films of α-chitin nanowhiskers/nanofibers obtained by TEMPO-mediated oxidation method, surface cationization of partially deacetylated chitin and conventional acid hydrolysis were studied and compared with those of squid-pen β-chitin nanofibers, as reported by Fan et al. [53].

The results suggested that squid-pen β-chitin nanofiber dispersion showed the highest shear stress and viscosity due to its highest aspect ratio, that the film of partially deacetylated α-chitin nanowhisker/nanofiber mixture showed the highest tensile strength and elongation at break owning to its relatively higher degree of

crystallinity combined with higher aspect ratio, and that all the samples showed similar thermal stabilities and oxygen permeabilities.

## 3.4 Preparation of Nano Chitin Whisker

Before the preparation of nano chitin whisker (NCW), chitin has to be isolated from the chitin producing parts of living animals, in which chitin does not occur alone, whereas, chitin always coexists with some other compounds. At present, the major sources of chitin in industry are the shell wastes of crabs and shrimps. The shell wastes are mainly made up of chitin (20–30 %), proteins (30–40 %), calcium carbonate (30–50 %), lipids and astaxanthin (less than 1 %) [54]. Preparation of nano chitin whiskers involves various steps e.g., preparation of raw chitin including isolation, demineralization, deproteinization and finally the extraction of nano chitin whiskers. The raw chitin is obtained from crustacean shells and mycelium of fungi following the detailed procedure given under the following headings:

### *3.4.1 Isolation of Chitin*

Chitin and chitosan do not occur in a pure or in an isolated form. A substantial effort has been made to develop chemical, mechanical, and enzymatic methods to obtain purified materials [54]. The usual method of obtaining chitin involves the chemical treatment of shellfish wastes from the crab and shrimp industries. The first step is to demineralize the shell with dilute hydrochloric acid at room temperature. This is followed by a deproteinization step with warm dilute caustic. This yields a partially deacetylated chitin, which may then be further deacetylated to chitosan. In actual practice the isolation of chitin from shellfish involves the step-by-step removal of the two major constituents of the shell, the intimately associated proteins by deproteinization and inorganic calcium carbonate by demineralization, together with small amounts of pigments, lipids and trace-metals leaving chitin as the final residue [55]. Many methods have been proposed and used over the years. The isolation of chitin begins with the selection of shells. Ideally, shells of the same size and species are chosen. For shrimp shells, the comparatively thin walls make recovery of chitin easier. The cleaning and drying of the shells followed by thorough crushing is the next step in the process. The small shell pieces are treated with dilute hydrochloric acid to remove calcium carbonate. Proteins as well as other organic impurities are removed by an alkali treatment (20 % sodium hydroxide). The pigments, primarily carotenoids are removed by extraction with ethanol or acetone after the demineralization process. A typical procedure of getting the raw chitin is outlined in Fig. 3.7.

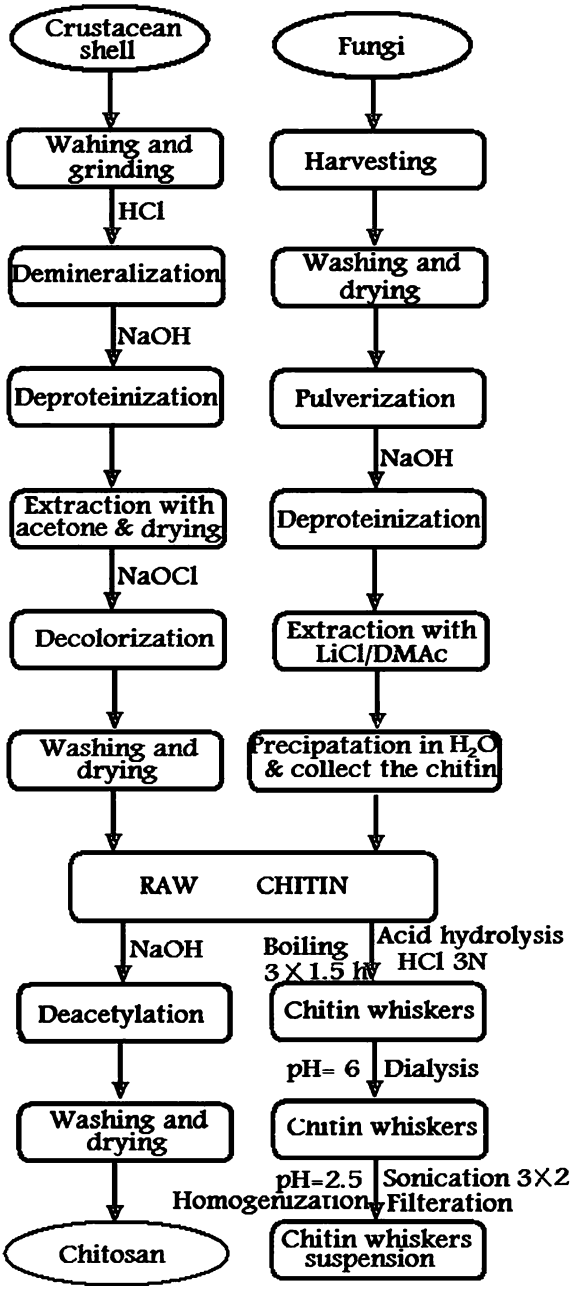


**Fig. 3.7** Schematic representations for the preparation of raw chitin and chitosan and chitin whiskers

### 3.4.2 Demineralization

Demineralization as the term suggests is the removal of minerals, primarily calcium carbonate. A mineral free chitin i.e. very low ash content chitin would be required for applications that have very low impurity tolerance. Demineralization is readily achieved because it involves the decomposition of calcium carbonate into the water-soluble calcium salts with the release of carbon dioxide. The extensively used reagent for this purpose is dilute hydrochloric acid (HCl) that produces water-soluble calcium chloride ($CaCI_2$). Some of the shortcomings of using HCl are that the large volumes of $CaCI_2$ solution must be disposed off and being a strong acid, can cause some hydrolysis of the chitin chains thereby reducing the molecular weight of the biopolymer. Performing demineralization at room temperature or lower can minimize this depolymerization of chitin chains.

### 3.4.3 Deproteinization

In deproteinization, covalent bonds between the chitin-protein complexes have to be destroyed. This is achieved with some difficulty especially if performed heterogeneously utilizing chemicals that will also depolymerize the biopolymer. The complete removal of protein, possible from shellfish sources, is especially important for biomedical applications. Chemical methods were the first approach used in deproteinization. A wide range of chemicals have been tried as deproteinization reagents including NaOH, $Na_2CO_3$, $NaHCO_3$, KOH, $K_2CO_3$, $Ca(OH)_2$, $Na_2SO_3$, $NaHSO_3$, $Ca(HSO_3)_2$, $Na_3PO_4$ and $Na_2S$. NaOH is the preferred reagent on the basis of its performance and typically a 1 M NaOH solution is used with variations in the temperature and duration of treatment parameters. The use of NaOH invariably results in partial deacetylation of chitin and hydrolysis of the biopolymer that lowers the molecular weight of chitin [50, 51]. Normally the protein content in the raw chitin produced from traditional commercial sources is around 1 %. In seeking to raise the deproteinization efficiency and an alternative to the harsh chemical treatment other methods have emerged and are being investigated. The use of proteolytic enzymes such as pepsin, papain or trypsin has been shown to minimize deacetylation and depolymerization in the chitin isolation. Other proteolytic enzymes such as tuna trypsin, Rhozyme-62, cod trypsin and bacterial proteinase have also been demonstrated the removal of proteins from crustacean shells. Bustos and Healy [56] have found that chitin obtained by deproteinization of shrimp shell waste using proteolytic microorganisms such as *Pseudomonas maltophilia, Bacillus subtilis, Streptococcus faecium, Pediococcus pentosaseus* and *Aspergillus oryzae,* had a higher molecular weight compared to chemically prepared chitin. A schematic representation for the preparation of raw chitin and chitosan from crustacean shells and fungi is outlined in Fig. 3.7.

### 3.4.4 Extraction of Nano Chitin Whiskers

There are various studies in the literature which discuss the extraction of nano chitin whiskers (NCWs) from raw sources [37–40]. Based on the procedure reported [37], the commercial raw chitin was dispersed into a 5 wt% KOH aqueous solution, and then boiled for 6 h with mechanical stirring to remove most of the proteins. The resultant suspension was conditioned at ambient temperature overnight under mechanical stirring followed by filtering and washing with distilled water for several times. Subsequently, the crude product was bleached with 17 g of $NaClO_2$ in 1 L of water containing 0.3 M sodium acetate buffer for 6 h at 80 °C, and then fully rinsed with distilled water. The crude product was finally dispersed into a 5 wt % KOH aqueous solution for 48 h to remove residual proteins followed by centrifugation to produce protein-free chitin. The resulting suspension was centrifuged at 3000 rpm for 20 min. Chitin whisker suspensions were prepared by hydrolyzing the purified chitin sample with boiling solution of 3 N HCl for 1.5 h under stirring. The ratio of 3 N HCl to chitin was 30 mL/g. After acid hydrolysis, the suspensions were diluted with distilled water followed by centrifugation (10,000 trs/min for 5 min). This process was repeated three times. Next, the suspensions were transferred to a dialysis bag and dialyzed for 24 h against distilled water until a pH 6 was reached. The pH was subsequently adjusted to 3.5 by adding HCl. The dispersion of whiskers was completed by a further 2.5 min ultrasonic treatment (B12 Branson sonifier) for every 40 mL aliquot. Morin and Dufresne [37] also prepared the nano chitin whiskers from Riftia. The diameter of these whiskers was 18 nm and length around 120 nm. In another study Gopalan and Dufresne [38] extracted nanochitin whiskers from crab shell. They successfully extracted 100–600 nm length and 4–40 nm width nanocrystal aggregate in the form of 500–1000 μm chitin microcrystal. Rujiravanit and coworkers [39] have reported preparation of chitin whiskers by acid hydrolysis of shrimp shells. The nanochitin whiskers consisted of slender rods with sharp points that had broad distribution in size. The length of the chitin fragments ranged from 150 to 800 nm, the width ranged from 5 to 70 nm. More than 75 % of the whiskers however, had a length below 420 nm. From the group of Zhang and coworkers [40] nanochitin whiskers were prepared from crab shell. It was spindle shaped with broad distribution in length (L) ranging from 100 to 650 nm and diameter (D) ranging from 10 to 80 nm.

### 3.4.5 Deacetylation of Chitin into Chitosan

Chitosan is prepared by hydrolysis of acetamide groups of chitin. This is normally conducted by severe repetitions of alkaline hydrolysis due to treatment due to the resistance of such groups imposed by the *trans* arrangement of the C2-C3 substituents in the sugar ring [57]. Thermal treatments of chitin under strong aqueous

alkali are usually needed to give partially deacetylated chitin (DA lower than 30 %), regarded as chitosan. The deacetylation of chitin into chitosan is usually achieved by treating chitin with 50 % NaOH at 95 °C for 3 h, cooling down, decanting off the NaOH and washing with water until neutral pH. This procedure is normally repeated twice. Finally the chitosan is extracted with 2 % acetic acid solution, filtered and precipitated in distilled water to give purified chitosan that is dried and stored. In general, two different methods for preparing chitosan from chitin with varying degree of acetylation are known. These are the heterogeneous deacetylation of solid chitin and the homogeneous deacetylation of pre-swollen chitin under vacuum in an aqueous medium. In both, heterogeneous and homogeneous conditions, the deacetylation reaction involves the use of concentrated alkali solutions and long processing times which may vary depending on the heterogeneous or homogeneous conditions from 1 to nearly 80 h. In practice, the maximal degree of deacetylation that can be achieved in a single alkaline treatment is about 75–85 % [58]. For better yield, during deacetylation, the conditions must be properlycontrolled in a reasonable time so that the chitin may be deacetylated tochitosan resulting in better yield.

Several alternative processing methods have also been developed to reduce the long processing times and large amounts of alkali typically needed to deacetylate chitin to an acid-soluble derivative. Examples of these include the use of successive alkali treatments using thiophenol in DMSO [59]; thermo-mechanical processes using a cascade reactor operated under low alkali concentration [60]; flash treatment under saturated steam [61]; use of microwave dielectric heating [62]; and intermittent water washing [63]. There is evidence that in certain bacteria and fungi, enzymatic deacetylation can take place [64]. Deacetylases have been isolated from various types of fungi, namely *Mucorrouxii*, *Aspergillus nidulans* and *Colletotrichum lindemuthianium.* However, the activity of these deacetylases is severely limited by the insolubility of the chitin substrate.

Recently a microwave technique for efficient deacetylation of chitin nanowhiskers to a chitosan nanoscaffold has also been reported [65]. A chitosan nanoscaffold in the form of a colloidal solution was obtained from the deacetylation of chitin whiskers under alkaline conditions by using a microwave technique in only 1/7 of the treatment time of the conventional method (Fig. 3.8). Fourier-

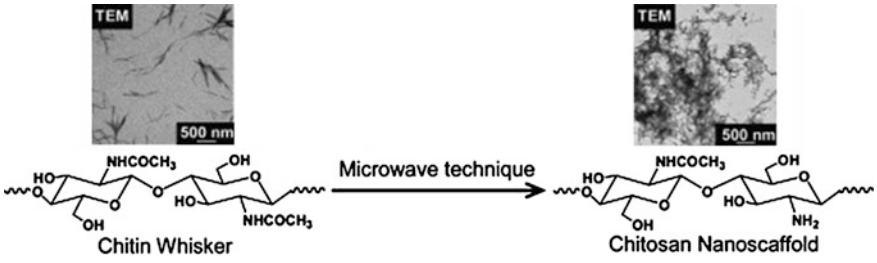


**Fig. 3.8** Efficient deacetylation of chitin nanowhiskers to a chitosan nanoscaffold using microwave technique [65]

transform infrared spectroscopy (FTIR) and nuclear magnetic resonance ($^1$H NMR) techniques confirm the degree of deacetylation to be above 90 % within 3 h. The wide-angle X-ray diffraction (WAXD) pattern clearly shows that the highly crystalline chitin whiskers are changed to amorphous chitosan. SEM micrographs show the aggregation of branched nanofibers, whereas the TEM micrographs reveal the scaffold morphology.

### 3.4.6 Chitosan Nanoparticles Preparation

For the purpose of chitosan nanoparticles preparation, 20 mg chitosan is dissolved in 40 ml of 2.0 % (v/v) acetic acid and 20 ml of 0.75 mg/ml tripolyphosphate TPP is dropped into a beaker at room temperature. After that chitosan solution was sonicated for 5 min and centrifuged for 15 min at 6000 rpm in order to obtain chitosan nanoparticles. These chitosan nanoparticles could be stored in distilled water; however, sonication for 10 s should be applied before a further immobilization step. The morphological characterization of the chitin whisker and chitosan nanoparticles can be evaluated by a Transmission Electron Microscopy (TEM) and Nanosizer.

### 3.4.7 Depolymerization of Chitosan

The main limitations in the use of chitosan in several applications are its high viscosity and low solubility at neutral pH. Low molecular weight (Mw) chitosans and its oligomers can be prepared by hydrolysis of the polymer chains. For some specific applications, these smaller molecules have been found to be much more useful. Chitosan depolymerization can be carried out chemically, enzymatically or physically. Chemical depolymerization (Fig. 3.9) is mainly carried out by acid

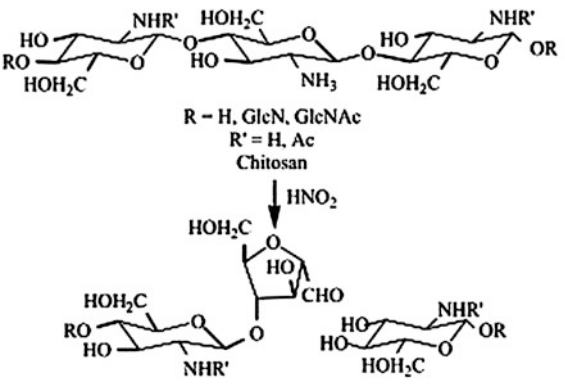


**Fig. 3.9** Chemical depolymerization of chitosan with $HNO_2$ [68]

hydrolysis using HCl or by oxidative reaction using $HNO_2$ and $H_2O_2$ [66]. It has been found to be specific in the sense that $HNO_2$ attacks the amino group of D-units, with subsequent cleavage of the adjacent glycosidic linkage. In case of enzymatic depolymerization, the low molecular weight chitosan with high water solubility can be produced by several enzymes such as chitinase, chitosanase, gluconase and some proteases. Non-specific enzymes including lysozyme, cellulase, lipase, amylase and pectinase that are capable of depolymerization of chitosan are known [67]. In this way, regioselective depolymerization under mild conditions is allowed. Physical depolymerization yielding dimers, trimers and tetramers has been carried out by radiation (Co-60 gamma rays) but low yields have been achieved [68].

## 3.5 Characterization of Nano Chitin Whiskers

For the determination of physicochemical characteristics of chitin and chitosan, various methods are available in the literature for the purpose. The detailed informations have been presented in the Table 3.2.

The chitin has been characterized by FTIR spectroscopy. The FTIR spectra of original chitin have also been discussed elsewhere [96]. However, FT-IR spectra of original chitin (Fig. 3.10) shows the broad OH stretching vibration band appeared at 3,443 $cm^{-1}$. The N–H symmetric and asymmetrical stretching vibration bands appeared at 3,289 and 3,105 $cm^{-1}$, respectively. The C–H symmetric and asymmetric stretching vibrations of $CH_2$ groups were observed at 2,931 and 2,889 $cm^{-1}$, respectively. The spectral region of 686–1,661 $cm^{-1}$ is the information-rich region. The faint absorptions at 1,661, 1,626 are due to C=O bond

**Table 3.2** Physicochemical characteristics of chitin and chitosan and the determination methods

| Sr. no. | Physical characteristics | Determination methods |
|---|---|---|
| 1 | Degree of deacetylation | Infrared spectroscopy [87, 218, 219] |
| | | First derivative UV-spectrophotometry [220, 221] |
| | | Nuclear magnetic resonance spectroscopy ($^1$HNMR) and ($^{13}$CNMR) [86, 87, 222, 223] |
| | | Conductometric titration [223] |
| | | Potentiometric titration [224] |
| | | Differential scanning calorimetry [225] |
| 2 | Average Mw and/or Mw distribution | Viscosimetry [226] |
| | | Gel Permeation chromatography [227] |
| | | Light scattering [216] |
| 3 | Crystallinity | X-ray Diffraction [228, 229] |
| 4 | Moisture contents | Gravimetric analysis [230] |
| 5 | Ash contents | Gravimetric analysis [230] |
| 6 | Protein | Bradford method [231] |

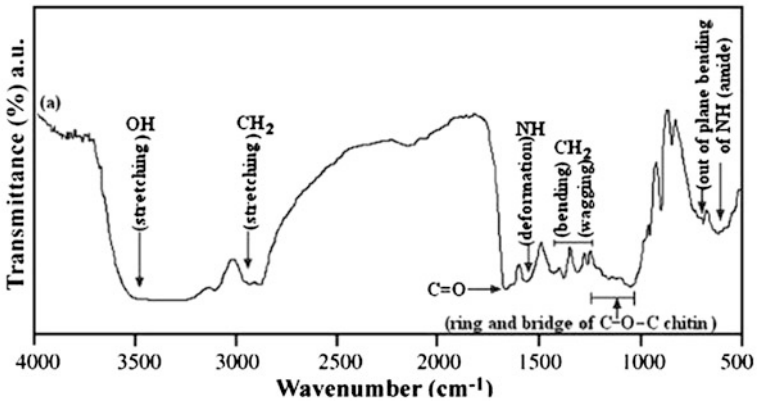


**Fig. 3.10** FTIR spectra of chitin [96]

and at 1,563 $cm^{-1}$ is due to NH deformations. The absorption bands at 1,427, 1,377 and 1,307 $cm^{-1}$ were attributed to $CH_2$ bending vibration, CH bending vibration and $CH_2$ wagging, respectively. The bands appeared at 1,261 and 1,204 $cm^{-1}$ are due to NH bending vibration and OH in-plane bending. The absorption band appearing at 1,158 $cm^{-1}$ is due to the asymmetric in-plane ring deformation. The absorption bands appearing at 1,046 and 1,026 $cm^{-1}$ are due to C–O and C–C stretching vibration. The two absorption bands at 950 and 896 $cm^{-1}$ are due to C–O ring vibration and ring bending. The broad intense band at 1,000–1,220 $cm^{-1}$ was attributed to the ring and bridge C–O–C vibrations of chitin-ether-type absorption. On the other hand, a weak shoulder at 710 $cm^{-1}$ and well-resolved band at 686 $cm^{-1}$ are assigned to the out-of-plane bending of NH (amide).

Transmission Electron Microscopy (TEM) is very good tool for characterizing the structure of nanosized materials. Nair and Dufresene [70] studied the colloidal suspension of chitin whiskers as the reinforcing phase and latex of both unvulcanized and prevulcanized natural rubber as the matrix. The chitin whiskers, prepared by acid hydrolysis of chitin from crab shell, consisted of slender parallel epiped rods with an aspect ratio close to 16. After the two aqueous suspensions were mixed and stirred, solid composite films were obtained either by freeze-drying and hot pressing or by casting and evaporating the preparations. Figure 3.11 shows TEM image of chitin whiskers obtained from crab shells.

Atomic Force Microscopy (AFM) is also another good tool for detecting the dimension of the nano sized particles. Oksman and coworkers [71] observed that AFM analysis of the chitin and cellulose whiskers is a good alternative to electron microscopy, without any limitations regarding contrast and resolution. The shape of the whiskers appeared, however, different from that observed in TEM. Scanning Electron Microscopy (SEM) is generally employed for the more extensive morphological inspection. It consists of the observation of fractured surface films at liquid nitrogen temperature. This technique allows for conclusions about the

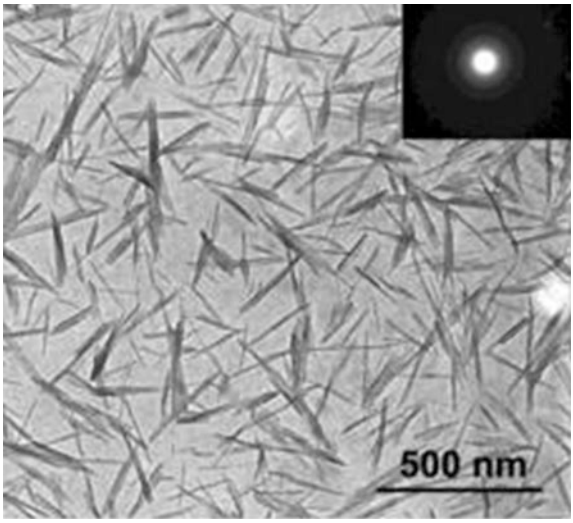


**Fig. 3.11** TEM image of chitin whiskers from crab shell [70]

homogeneity of the composite, presence of voids, dispersion level of the whiskers within the continuous matrix, presence of aggregates, sedimentation, and possible orientation of whiskers. Their diameter determined by SEM is much higher than the whiskers diameter. This results from a charge concentration effect due to the emergence of cellulose whiskers from the observed surface. Gopalan et al. [72, 73] have extracted nano chitin whiskers from crab shell. Figure 3.11 shows a transmission electron micrograph of a dilute aqueous suspension of hydrolyzed crab shell chitin. The suspension contains chitin fragments consisting of both individual micro crystals and associated or collapsed micro crystals. These chitin fragments consist of slender rods with sharp ends that have a broad distribution in size. Rujiravanit and coworkers [41] also showed the size of chitin whisker from shrimp shells by using TEM. Michel and Dufresne [74] also showed transmission electron micrographs of nano chitin whiskers from squid pen chitin. AFM analysis of the whiskers was found to be a good alternative to TEM without any limitations regarding contrast and resolution. The shape of the whiskers appeared, however, different than that observed in TEM and FESEM.

X-ray diffraction (XRD) is a versatile, non-destructive technique that reveals detailed information about the chemical composition and crystallographic structure of natural and manufactured materials. Zia et al. [96] reported that the crystalline structure of chitin with dimension $a = 4.85$ Å, $b = 9.26$ Å, $c = 10.38$ Å (fiber axis), and $\gamma = 97.5°$. The unit cell contains two sugar residues related by the two fold screw axis. The structure contains extended polymer chains indicating an anti-parallel arrangement of the chitin chain with strong intermolecular hydrogen bonding [75]. Five crystalline reflections were observed in the $2\theta$ range of 5–30° (Fig. 3.12).

The observed patterns of the crystalline peaks in the $2\theta$ range were indexed as 9.39°, 19.72°, 20.73°, 23.41° and 26.39° for the lower angle for chitin. The outcomes of the results are in accordance with the previous findings [75–77].

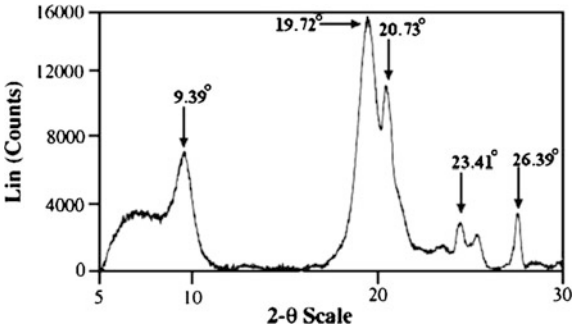


**Fig. 3.12** XRD pattern of chitin [96]

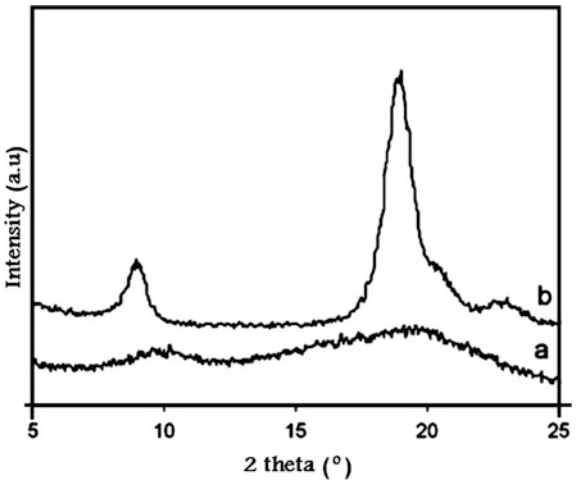


**Fig. 3.13** X-ray analysis data of chitosan/chitin crystal nanocomposites

As shown in Fig. 3.12 exhibited a broad signal centered at $2\theta = 19.72°$, which is attributed to the GlcN sequences. Similarly, the intensity of the broad signal centered at $2\theta = 9.39°$ due to GlcNAc sequences [78].

Very recently Mathew et al. [79] reported on the crystal studies of chitosan/chitin crystal nanocomposites. The chitosan (a) exhibits a highly amorphous nature with broad and ill-defined signals at $2\theta = 9–10°$ and 18–20° (Fig. 3.13). The chitin nanocrystals (b) show a strong peak at $2\theta = 8.8$ and 19° and shoulders at $2\theta = 20$ and 22°, confirming its crystalline structure as $\alpha$-chitin.

### *3.5.1 Characterization of Chitin and Chitosan for Medicinal Applications (Medical Devices)*

It is necessary to prepare several tests, grouped in preliminary, confirmatory and other tests, for characterization of chitin and chitosan used for manufacturing of medical devices [80]. European Pharmacopoeia as well as requirements of ISO

10993-18:2005 [81] and ISO/DIS 10993-1910 [82] Standards for the determination of range of analytical characterization of chitosan must be taken into consideration.

1. *Moisture content and form identification*

Usually moisture contents of chitosan vary from 5.0 to 15.0 % which results changing with humidity and form of chitosan (flakes or powder). The form of the biopolymer is able to give suitable information for quality. The sample of biopolymer should be suspended in water, filtered and dried for detection of water-soluble contaminants.

2. *Ash and protein content in chitosan*

Protein and ash content of chitosan are very important parameters and those should be investigated early in the quality assay protocol. A high quality grade product should have less than 1 % of protein as well as ash content.

3. *Insolubility, turbidity, color and UV absorption of chitosan solution*

For determination of insolubility, turbidity, color and UV absorption of chitosan 1 % (w/v) solution of dried sample ought to be prepared in 1 % acetic acid solution. When the sample is dissolved, the solution is filtered and insolubility of the sample is determined. The insolubility of a good quality chitosan should not exceed 0.1 %. If the appearance of the residues is different from that of chitin and chitosan, one may consider analyzing its nature. The turbidity of 1 % sample solution in 1 % acetic acid should be less than 15 NTU (i.e., nephelometric turbidity units) and should be free from physical contamination by visual examination. The transmittance should be higher than 90 %, both at $\lambda = 400$ nm and $\lambda = 560$ nm. The UV spectrum of chitosan is additionally able to provide the other chromophoric impurities information upon the interference of other chromophores. If during preliminary tests no significant deviation has been found, then further investigations should be conducted for the confirmatory test.

4. *Confirmatory test: Chromatographic and spectroscopic examinations*

Acid hydrolysis of chitosan followed by the HPLC detection of the amount of acetic acid liberated is able to give acetyl content of chitin/chitosan. Due to the high sensitivity, availability, easiness of method and effectiveness in detection of functional groups IR spectroscopy can give useful information about the acetyl content of chitin/chitosan as well as possible cross-contaminations. The results of Differential Thermogravimetric Analysis (DTA) show increased thermostability compared to GlcNAc. Discussed biopolymer shows its main thermal process from 275 to 280 °C respectively.

5. *Further confirmation tests*

In general, one can assure the confirmatory test for chitosan after colorimetric analysis since above-mentioned series of physical and chemical analysis can clearly investigate the identity of sample. But in certain cases, one might encounter

to check the purity of chitosan for very sensitive applications that demand very high purity. Then, NMR spectroscopy will come into consideration as described in ISO 10993-18:20059 and ISO/DIS 10993-1910 Standards [82].

6. *Other characteristics of chitosan*

The remaining parameters of chitosan should be taken into the consideration. Molecular weight of chitosan is one of the important properties affecting chitosan quality and reproductively of results in several medicinal applications requires different range of molecular weights or strictly narrow range of molecular weight. X-ray diffraction is a perfect analytical method to define the crystallinity but IR and NMR spectra are able to provide additional data for intrepretation and understanding sample morphology. Not only heavy metals but nitrogen, chloride, ammonia contents in chitosan are also very important in medical applications. Additionally, extractable residues in non-polar and polar solvents are helpful in identifying the characteristic of investigated samples. Source for manufacture of medical devices should be apyrogenic as well as it should not contain pathogenic contamination. Therefore, it is useful to determine biological contamination defined as viable aerobic microorganisms, fungi, mould and yeast content. The bioburden level should be measured before introduction of new portion of source for production to avoid accidental cross-contamination.

## 3.6 Manufacture of Chitin Nanocomposites and Blends

Morin and Dufresne [37] prepared nanocomposites from a colloidal suspension of high aspect ratio chitin whiskers as the reinforcing phase and poly ($\varepsilon$-caprolactone) as the matrix. The chitin whiskers, prepared by acid hydrolysis of Riftia tubes, consisted of slender parallel-tubed rods with an aspect ratio close to 120. Films were obtained by both freeze-drying and hot-pressing or casting and evaporating the preparations. Amorphous poly (styrene-co-butyl acrylate) latex was also used as a model matrix. In another work [72] nanocomposite materials were obtained from a colloidal suspension of chitin whiskers as the reinforcing phase and latex of both unvulcanized and prevulcanized natural rubber as the matrix. The solid composite films were obtained either by freeze-drying and hot-pressing or by casting and evaporating the preparations. In another study, Lu et al. [38] prepared environment friendly thermoplastic nanocomposites using a colloidal suspension of chitin whiskers as a filler to reinforce soy protein isolate (SPI) plastics. SPI of desired weight and various contents of chitin were mixed and stirred to obtain a homogeneous dispersion. The dispersion was freeze-dried, and 30 % glycerol was added. The resulting mixture was hot-pressed at 20 MPa at 140 °C for 10 min and then slowly cooled to room temperature. Rujiravanit and coworkers [83] prepared $\alpha$-chitin whisker-reinforced poly (vinyl alcohol) (PVA) nanocomposite films by solution-casting technique. Casting technique leading to the formation of films was used for the preparation of latex based starch nanocomposites [84]. In another

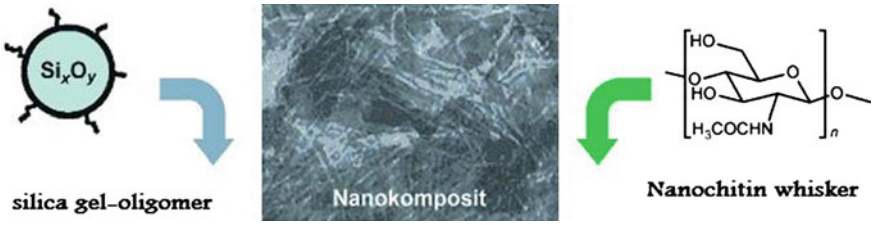


**Fig. 3.14** Self-organization and sol–gel chemistry of colloids for the formation of chitin-silica nanocomposites [85]

study Alonso, et al. [85] prepared chitin-silica nanocomposites by self-organization. Self-organization processes of chemical building blocks are the basis for many biological processes (Fig. 3.14).

The synthesis was carried out by sol–gel process techniques. The sol into a desired shape can be "cast" and dried. So a nanocomposite formed from silicon dioxide into a fully-integrated matrix of chitin rods. The mechanism is based on a self-organized storage of chitin and weak forces of attraction between chitin and siloxane oligomers. Different textures and morphologies are accessible by adjusting the evaporation process or by applying external fields.

In another study Feng et al. [86] presented the structure and properties of new thermoforming bionanocomposites based on chitin whiskers-graft-polycaprolactone. The synthesized material was characterized by FTIR, SEM, TEM and XRD. The surface and mechanical properties were also determined and discussed. Hariraksapitak et al. [87] prepared a neat hyaluronan–gelatin scaffolds and chitin-whisker-reinforced hyaluronan–gelatin scaffolds. The obtained cylindrical scaffolds obtained were about 10 mm in diameter and 2 mm in height, whereas the disc-shaped scaffolds were about 1 mm in thickness; these were later cut into a desired shape and size for the mechanical property assessment.

Eectron beam is usually used on the polymeric material to induce effects such as chain scission (which makes the polymer chain shorter) and cross linking. The result is a change in the properties of the polymer which is intended to extend the range of applications for the material. The effects of irradiation may also include changes in crystallinity as well as microstructure. Usually, the irradiation process degrades the polymer. The irradiated polymers may sometimes be characterized using DSC, XRD, FTIR, or SEM. In poly(vinylidene fluoride-trifluoroethylene) copolymers, high-energy electron irradiation lowers the energy barrier for the ferroelectric-paraelectric phase transition and reduces polarization hysteresis losses in the material [88].

Electron beam irradiation is an alternate method to prepare poly(aniline) (PANI) nanocomposite stable at ambient conditions. Ramaprasad et al. [89] synthesized the chitin-polyaniline nanocomposite by electron beam irradiation method (Fig. 3.15). The blends of chitin and PANI with PANI 30, 50, and 70 % (30P, 50P, and 70P) were prepared by mixing 0.5 % (wt%) chitin solution and 0.5 % (wt%) EB solution in DMA with 5 % LiCl in required proportions and irradiated with

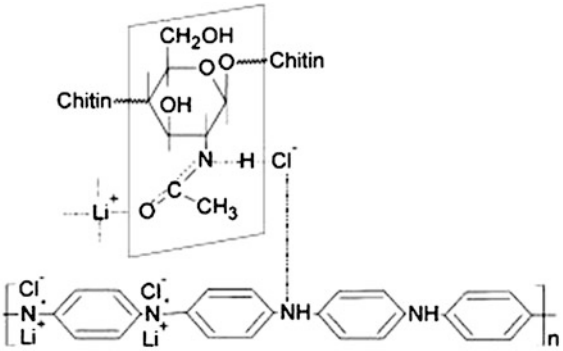


**Fig. 3.15** Interaction between chitin and polyaniline [89]

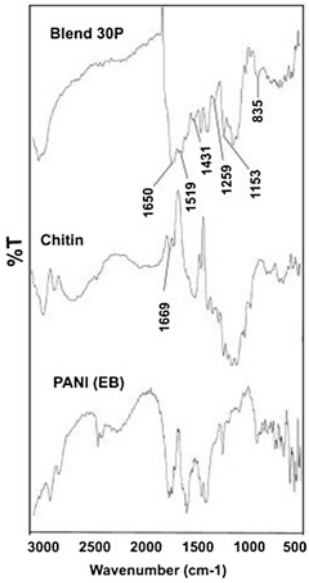


**Fig. 3.16** FTIR spectra of PANI (*EB*), chitin and 30P blend [89]

electron beam. During irradiation, the color of the solution turned blue to brown and above 4 kGy, immediately after the irradiation of blend solution, brown particles were obtained at the top of the solution, and after 20–30 min these particles were uniformly distributed in solution. The FTIR spectra of PANI, chitin, and 30P blend is presented in Fig. 3.16.

Preparations of $SiO_2$-chitin/carbon nanotubes (CNTs) bionanocomposites have also been reported by many researchers [90]. The use of nanomaterials such as CNTs to fabricate matrices for biosensors is one of the most exciting approaches because nanomaterials have a unique structure and high surface to volume ratio [90]. The surfaces of nanomaterials can also be tailored in the molecular scale in order to achieve various desirable properties [91]. The diverse properties of nanocomposite materials such as unique structure and good chemical stability enable them to provide a wide range of applications in sensor technology [92].

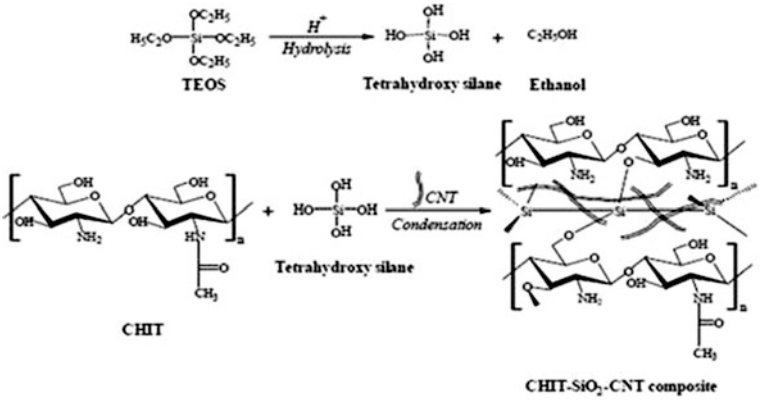


**Fig. 3.17** Reaction scheme for the preparation of $SiO_2$-chitin/CNTs bionanocomposites [90]

Moreover, the nanocomposites do not suffer from the drawback of sensing complications, synthesis complexities; have a long shelf life, and excellent performance. In to this addition, the fundamental electronic characteristics of CNTs could also be used to facilitate the uniform distribution within the nanocomposite biosensing electrodes. There are many reports on integration of CNTs with sol–gel derived $SiO_2$-chitin to fabricate biosensors to gain synergistic action using organic–inorganic bionanocomposites. The sol–gel $SiO_2$-chitin is prepared by mixing of alcoholic silica precursor such as tetraethyl orthosilicate (TEOS) and chitin solution under magnetic stirring at room temperature. To this mixture, homogeneously dispersed CNTs in ethanol are added. The mixture initially comprising of two phases is made uniform by stirring vigorously until -$SiO_2$ is distributed evenly in the aqueous solution while the hydrolysis reaction occurs. After certain time period, the opaque and black sol is formed (Fig. 3.17). In a controlled process, tetraethoxysilane undergone hydrolysis and formed tetrahydroxy silane (silanol) at acidic pH [93]. The resulted silanol then reacted with chitin via a condensation reaction between the -OH groups and led to the formation of a chitin-$SiO_2$ composite network, in which CNTs are homogeneously dispersed. Both CNTs and $SiO_2$ improve the mechanical properties of the chitin-$SiO_2$-CNTs bio- nanocomposite, primarily CNTs enhance the electrical conductivity of the bio- composite.

The fabrication of enzyme-$SiO_2$-Chitin-CNT bioelectrodes have also been reported [94]. The $SiO_2$-chitin/CNTs sol thin film is fabricated by spreading it uniformly onto a substrate such as ITO glass plate (i.e., indium tin oxide coatings on *glass* slides) using spin coating technique and subsequently dried at room temperature. $SiO_2$-chitin/CNTs/substrate electrode is washed with deionized water followed by phosphate buffer saline of pH 7.0 in order to maintain pH over the electrode surface. $SiO_2$-chitin/CNTs electrode is treated with aqueous glutaraldehyde as a cross-linker. The freshly prepared enzyme solution is uniformly spread onto glutaraldehyde treated $SiO_2$-chitin/CNTs electrode and is kept in a humid

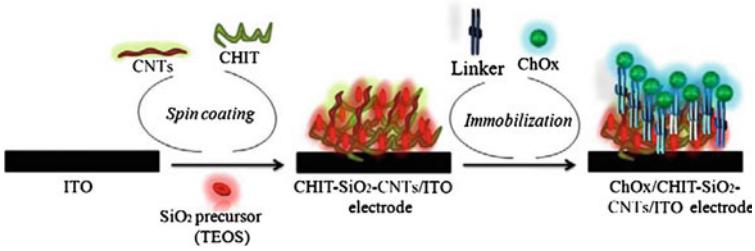


**Fig. 3.18** Schematic diagram of the fabrication of CHIT-$SiO_2$-CNTs/ITO and ChOx/CHIT-$SiO_2$-MWNT/ITO electrodes

chamber at 4 °C for 12 h, Fig. 3.18. The enzyme-$SiO_2$-chitin/CNTs bioelectrode is immersed in phosphate buffer solution of pH 7.0 in order to wash out unbound enzyme from the electrode surface.

Extensive work on detailed molecular characterization [95], XRD studies [96], and thermal properties [96] of chitin-based polyurethane elastomers (PUEs) have also been extensively studied and reported in the literature. In vitro biocompatibility and non-toxicity of chitin/1,4-butanediol blends based polyurethane elastomers has also been reported elsewhere [97, 98]. Some reports are also available on molecular characterization and shape memory properties of chitin-based shape memory polyurethane elastomers [99, 100]. For the application of PU, their stability against terrestrial weathering is important. One of the greatest factors in the terrestrial weathering of PUEs is ultraviolet (UV) radiation in the wave-length range 330–410 nm. Attempts have also been made to study the effect of UV-irradiation on surface properties of some common polymers [101–103]. Photo-oxidative behavior and effect of chain extender length in polyurethane on photo-oxidative stability have also been reported [104]. Surface morphology of starch [105], cellulose [106], and chitin–humic acid [107] have also been investigated and well documented. XRD studies and surface characteristics of UV-irradiated and non-irradiated chitin-based polyurethane elastomers have also been presented in different research articles [108–110]. The synthesis and characterization of chitin based polyurethane samples have been reported using chitin as chain extender/crosslinker [116. 132]. The synthetic scheme for the synthesis of chitin based polyurethane is presented in Fig. 3.19.

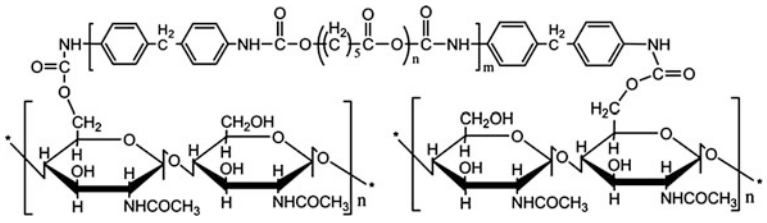

**Fig. 3.19** Synthesis of chitin based polyurethane [100]

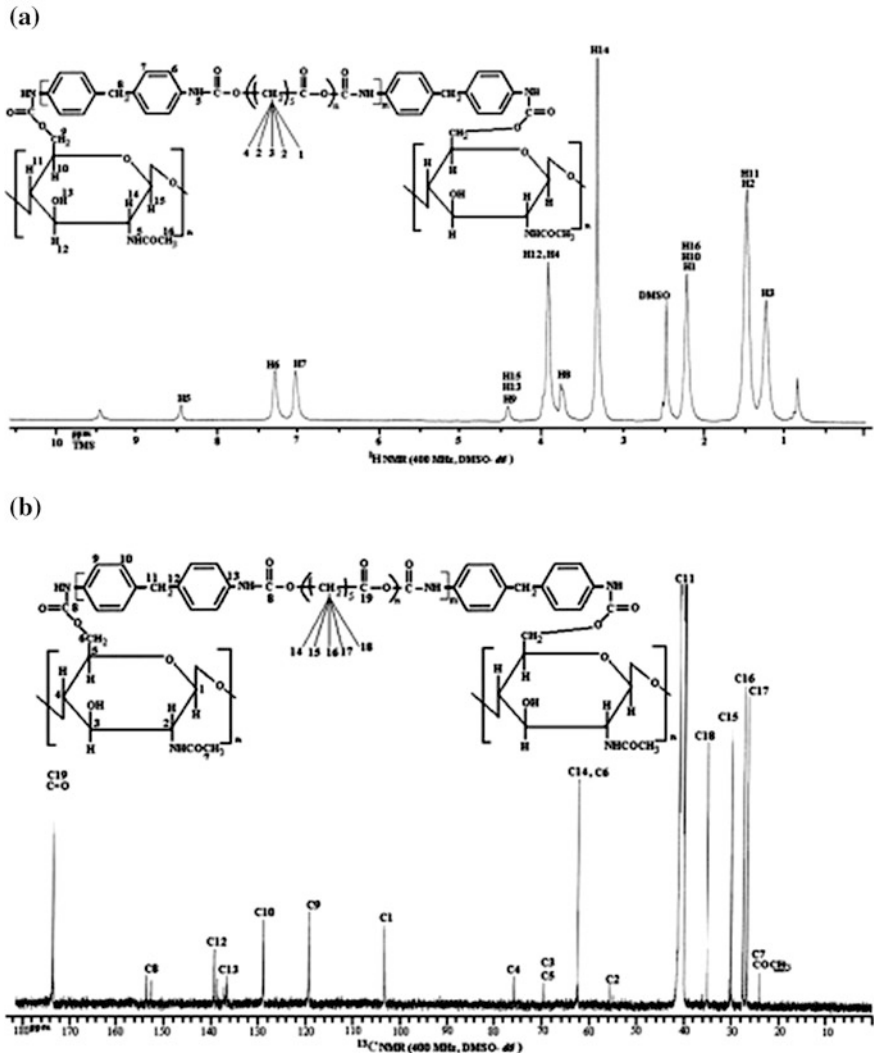


**Fig. 3.20** **a** $^{1}$H NMR. **b** $^{13}$C NMR spectra of chitin based polyurethane [95]

The $^{1}$H NMR and $^{13}$C NMR spectra of final synthesized chitin based polyurethane (PU) samples were in accordance with proposed structures (Fig. 3.20). $^{1}$H NMR spectra obtained for chitin based PU exhibited new peaks at 4.48 ppm which was assigned to the proton of C1, C3 and C6 position of chitin. $^{13}$C NMR spectra obtained for the chitin-based PU samples, exhibited peaks at 23.0 and 174 ppm, which were attributed, respectively to the $CH_3$ (methyl) and C=O (carbonyl) group of chitin [111]. Moreover, the peaks located at about 56.2, 63.3, 69.6, 68.8, 77.5 and 104 ppm were attributed to C2, C6, C3, C5, C4 and C1 positions of chitin,

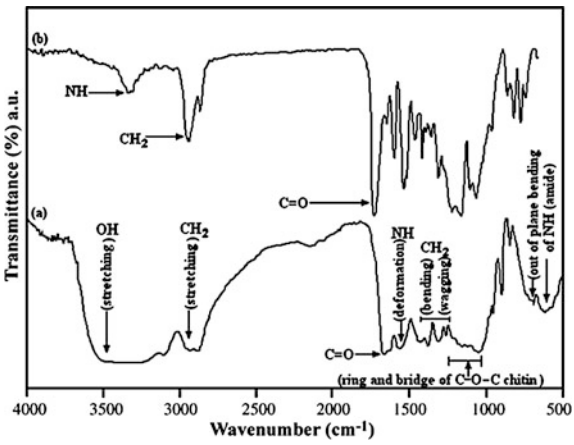


**Fig. 3.21** FTIR spectra of **a** original chitin, **b** NCO-terminated pre-polymer extended with chitin [114]

respectively [112, 113], which provides evidence of involvement of chitin in final polyurethane structure. The FTIR spectra confirm the synthesis of chitin based polyurethane. The FTIR spectra of original chitin and polyurethane extended with chitin are shown in Fig. 3.21a and b.

The role chitin as a material of highly ordered crystalline structure has been reported in the study [96]. X-ray diffraction analysis was carried out in order to find the changes of the crystalline structure upon the substitution reaction with NCO terminated prepolymer. The X-ray diffraction studies showed that crystallinity mainly depends on the concentration of chitin in the polyurethane backbone, crystallinity increased as the concentration of chitin into the final PU increased (Fig. 3.22). The crystallinity of some polymers was clearly observed by optical microscopic studies [114]. The results of X-ray diffraction experiments correlate with optical microscopy findings. A crystalline polymer is distinguished from an amorphous polymer by the presence of sharp X-ray lines superimposed on an amorphous halo. Under an optical microscope, the presence of polycrystalline aggregates appear as spherulites [114]. The spherulites are made of small crystallites and grow from a nucleus at their centre. They consist of narrow chain folded lamellae growing radially. Since the fibrous crystals are radial, the chains folded with the lamellae are circumferentially oriented. From the evaluation of the X-ray and optical microscopic studies, it has been observed that the involvement of chitin in the PU formulation and have improved crystallinity of the final polyurethane.

The cell culture tests were used to evaluate both cytotoxicity and cytocompatibility of the specimens. In the cell culture method, the performance of a cell is investigated by comparing it with a negative control. A control is a sample thoroughly compatible with cells and is cultured with the main samples. A material is considered to be biocompatible, if it supports cell attachment and growth.

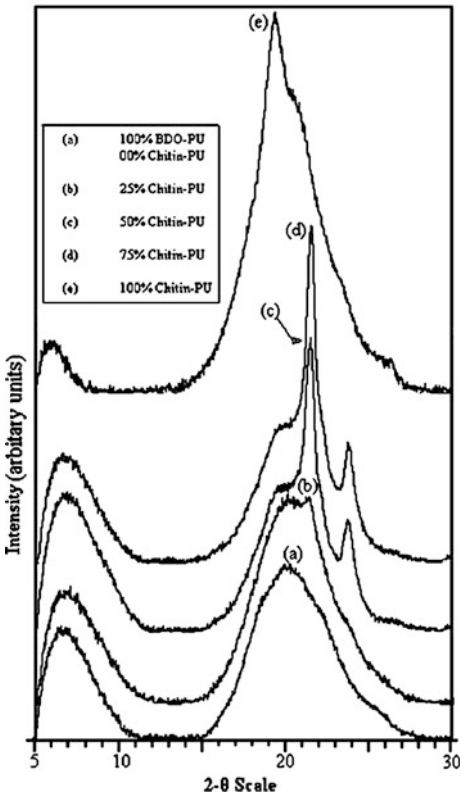


**Fig. 3.22** X-ray diffractograms of **a** CPU1–0 % chitin–PU, **b** CPU2–25 % chitin–PU **c** CPU3–50 % chitin–PU **d** CPU4–75 % chitin–PU **e** CPU5–100 % chitin–PU [96]

Zuber, et al. [115] prepared chitin based polyurethane bionanocomposites (PUBNC) by solution polymerization. The formation of well dispersed ordered intercalated assembled layers of bentonite in PU matrix was observed. The results revealed that pure silicate disappears in PU/bentonite nanoclay hybrid and a set of new peaks appear corresponding to the basal spacing of PU/bentonite clay bionanocomposites. Wang et al. [116] reported the synthesis of chitosan-based nanocomposites with montmorillonite. The nanocomposites were prepared by the solution intercalation method in which the chitosan solution was added to the clay dispersion followed by film casting. Morphology and properties of the composites generated with and without acetic acid residue were also compared with the pure polymer. Figure 3.23 shows the TEM micrographs of the composites with varying extents of montmorillonite. It was observed that the dispersion of filler was uniform. At low filler amounts, the morphology was of intercalated-exfoliated type. On the other hand, increasing the filler content led to the shift of morphology to mostly intercalate with occasional flocculation. The thermal performance of the nanocomposites was observed to be better than that of pure polymer. Higher

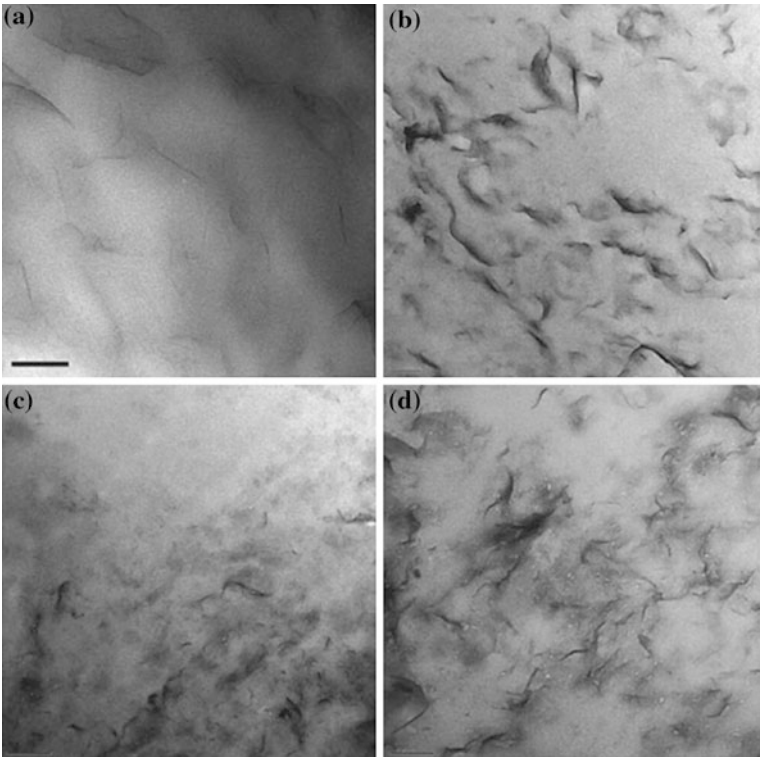


**Fig. 3.23** TEM micrographs of chitosan nanocomposites with **a** 2.5 wt % filler, **b** 5 wt % filler, **c** 5 wt % filler as well as acetic acid residue, and **d** 10 wt % filler [116]

hardness and superior mechanical properties were also observed in the composites as compared to pure polymer.

Darder et al. [117] also reported chitosan intercalated montmorillonite nanocomposites. Darder et al. [118] further reported on the reinforcement of chitosan with sepiolite, which is a natural magnesium silicate with micro fibrous texture. The study suggested a considerable interaction between hydroxyl groups belonging to the biopolymer structure of the chitosan polymer and the silanol groups present on the external surface of sepiolite as shown in Fig. 3.24. The crystalline structure of sepiolite was observed to be preserved during the nanocomposite synthesis. Strong interaction between the organic and inorganic components of the system was also confirmed with different characterization methods. The resulting composites were thermally more stable than the pure polymer. As a result of the strong interaction, the mechanical properties of the composites were also superior to those of the pure polymer. Similarly, other fillers like double layer hydroxides have also been incorporated in the polymer matrices [119].

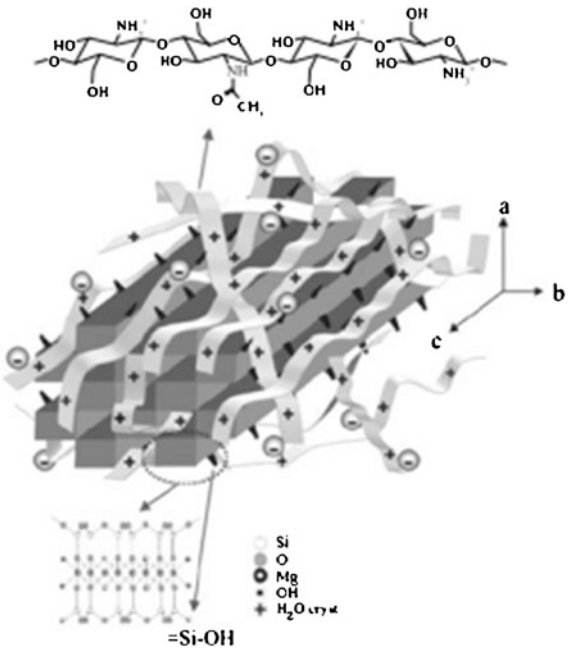


**Fig. 3.24** Representation of the chitosan adsorption on sepiolite surface [118]

### *3.6.1 Chitosan Based Nanocomposites*

Recently, much attention has been paid to chitosan as a potential polysaccharide resource due to its excellent properties [120–124]. The polymorphism of chitosan has also been studied, extensively and different conclusions have been drawnunder different study conditions. Nanocomposites based on the intercalation of chitosan in $Na^+$ montmorillonite are known to be robust and stable three-dimensional materials, since the interaction of the biopolymer with the clay substrate strongly reduces its film-forming tendency. When the chitosan amount exceeds the cationic exchange capacity (CEC) of the clay, the biopolymer is intercalated as a bilayer in the clay interlayer space by means of cationic exchange and hydrogen bonding processes. It was assumed that the excess of $–NH_3^+$ groups, which do not interact electrostatically with the negatively charged sites of the clay, is balanced with the acetate ions from the initial chitosan solution, providing the bidimensional nanostructured material with anionic exchange sites ($–NH_3^+X$). Since chitosan–montmorillonite nanocomposites exhibited good functional and mechanical properties, they were employed in the construction of bulk-modified sensors for the detection of anions [125]. In another study, ionotropic crosslinking methodology was used to synthesize chitosan-tripolyphosphate chelating resin beads to fabricate zero-valent copper-chitosan nanocomposites. The copper nanoparticles were dispersed on chitosan-tripolyphosphate beads, and were thus able to maintain appropriate dispersion and stability, which greatly improved their applicability. The fabrication process contains two steps: using chitosan-tripolyphosphate beads

to adsorb Cu(II) ions, followed by chemical reduction to reduce Cu(II) ions to zero-valent copper [126]. Huang et al. [127] synthesized various metal–chitosan nanocomposites including silver (Ag), gold (Au), platinum (Pt), and palladium (Pd) in aqueous solutions. Metal nanoparticles were formed by reduction of corresponding metal salts with $NaBH_4$ in the presence of chitosan. $Cu_2O$/CS nanocomposites are prepared by electrochemical deposition. By the joint analysis of photocatalytic performance of $Cu_2O$/CS nanocomposites with variant mass ratios of $Cu_2O$ in the decoloration of reactive brilliant red X-3B, and the chelation capability of CS and found that when the mass ratio of $Cu_2O$ in the $Cu_2O$/CS nanocomposites is 50 %, the composites provide with a new feasibility to eliminate the pollutants by visible light irradiation in the advanced treatment of drinking water [128]. The growth of hydroxyapatite (HA) on gelatin–chitosan composite capped gold nanoparticles was done for the first time by employing wet precipitation methods and obtained good yields of HA. High Resolution Transmission Electron Microscope images (HRTEM) of GC–Au–HA nanocomposites showed the size of nanocomposite about 50 nm [129]. Chitosan and chemically modified chitosan (CMC) were chosen matrices for synthesizing and stabilizing the gold, silver and platinum nanoparticles [130]. It was observed that CMC was poor choice as the nanoparticle aggregation and also lack of free amines limited the extent of polymer crosslinking. Lui and Huang in their work on nanocomposites of genipin (excellent natural cross-linker for proteins, collagen, gelatin,and chitosan) crosslinked chitosan silver nanoparticles concluded that silver nanoparticles affect the material characteristics, biological activity and antimicrobial activity. Enhanced micro-structural property of the nanocomposites reduced the biodegradation rate under enzymatic digestion [130].

Molecularly imprinted polymer (MIP) represents a new class of materials that have artificially created receptor structures. This potential technology is a method for making selective binding sites in synthetic polymers by using a molecular template. MIPs have steric and chemical memory toward the template and hence could be used to rebind it (Fig. 3.25).

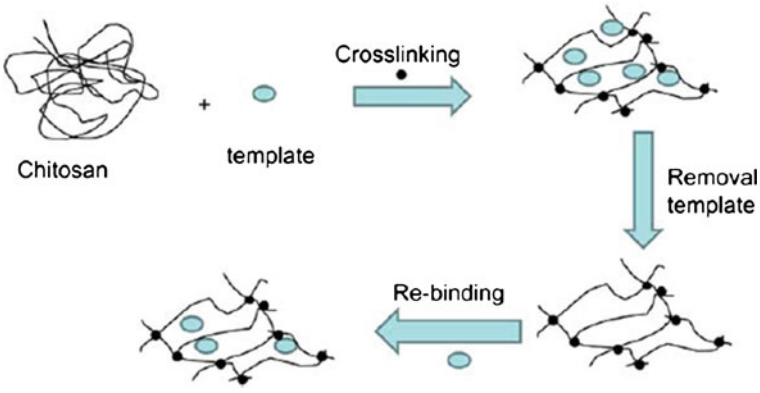


**Fig. 3.25** Schematic representation of imprinted chitosan-based matrix preparation [130]

### 3.6.2 Bionanocomposites: From New Sources to New Processes

In recent years a number of research studies on the synthesis of clay-based nanocomposites have been reported [112]. Nanocomposites, by virtue of the interactions between the organic and inorganic components, can have different morphologies [131]. In the intercalated morphology, the clay layers are still ordered. However, the exfoliated or delaminated morphology provides maximum benefit as the filler is completely delaminated and the platelet ordering is lost. This morphology has maximum interfacial contact with the polymer; thus, polymer properties like mechanical performance, barrier properties and biodegradability are significantly affected. Nanocomposites have also been prepared by different synthetic routes [132, 133]. In situ polymerization for preparation of nanocomposites, as described in the earlier section, is based on the swelling of the clay in the monomer followed by polymerizing the monomer in the presence of clay, thus trapping the delaminated clay in the polymer structure. Melt intercalations, also described earlier, is the method where the preformed high molecular weight polymer can be directly used for the synthesis of the polymer nanocomposite. In this case, the polymer is melted at high temperature, and the filler is slowly added to this melt under shearing in the compounder. The filler platelets are sheared during compounding and kneading in the compounder and thus are well mixed with the polymer phase. Another method for synthesizing polymer nanocomposites is solvent intercalation. In this case, the polymer is dissolved in the same solvent in which the clay is dispersed. Evaporation of the solvent leads to entrapment of the polymer chains in between the filler platelets. One can also synthesize thermoset polymer nanocomposites by this route. The prepolymer is dissolved in the solvent in which the filler is dispersed. The crosslinking is then initiated by the addition of the crosslinker. The simultaneous evaporation of solvent and crosslinking of the polymer matrix leads to delaminated filler in the polymer matrix. A more comprehensive review has been reported by Bordes et al. [134].

### 3.6.3 Polymer/Chitin Whisker Bionanocomposites Processing

Similar to cellulose nanocrystals, chitin whiskers also showed high values of different modulii. The longitudinal modulus and transverse modulus of the CW are 150 and 15 GPa, respectively. Thus, CWs can be used as potential nanofillers in reinforcing polymer nanocomposites. Following the use of cellulose nanocrystals in reinforcing poly(styrene-co-butyl acrylate) (poly(S-co-BuA))-based nanocomposites in 1995, the application of polysaccharide nanocrystals in reinforcing polymer nanocomposites have attracted a great deal of interests due to their appealing intrinsic properties [135–139]. Paillet et al. [36] first time reported the use of CWs in reinforcing thermoplastic nanocomposites in 2001, the same polymer, poly(S-co-BuA), was used as the matrix for the nanocomposites.

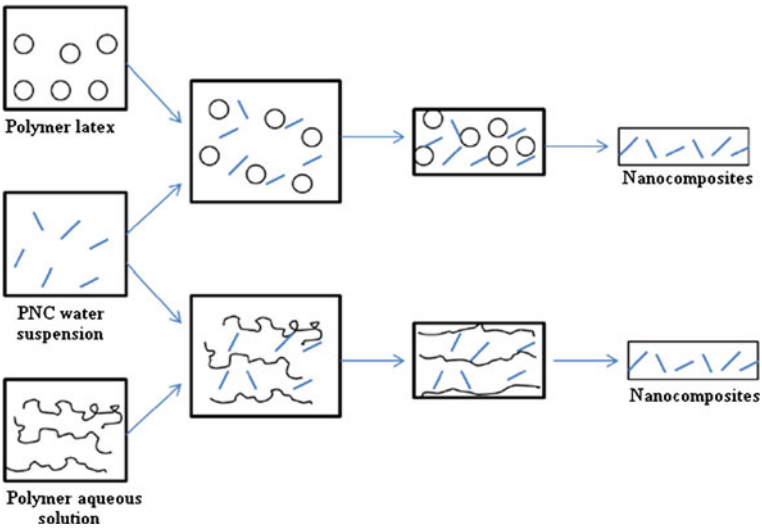


**Fig. 3.26** Casting-evaporating procedures for preparation of polymer/CW nanocomposites

Thereafter, CWs have been increasingly used in many other polymer matrices. Following processing steps are involved in the manufacturing of polymer/chitin whisker bio nanocomposites.

1. *Casting and evaporating technique*

The processing techniques have an important influence on the final properties of nanocomposites. The techniques that are employed should take into account the intrinsic properties of CWs, the nature of polymer matrix, and the desired final properties of the composites. Good dispersibility of CWs in polymer matrix is the prerequisite to prepare high performance polymer/CW nanocomposites. So for uniform composition CWs are homogenously dispersed in water and are usually obtained as aqueous suspensions. Thus, water is the best medium for preparation of CWs reinforced nanocomposites, and most investigations preferred to use water-soluble, water-dispersible and latex-form polymers as the polymer matrixes to make nanocomposites. In the process, as shown in Fig. 3.26, the polymer aqueous solution or dispersion was first mixed with CW aqueous suspension to obtain homogenous dispersion which was then casted onto a container; afterwards, the nanocomposites with CWs incorporated into polymer matrix were obtained by evaporation of water, this method is so-called casting and evaporating technique.

Most of the recent reported polymer/CW nanocomposites were prepared by this method. The reported polymer matrixes contain poly(styrene-co-butyl acrylate) [36], poly(caprolactone) [37], natural rubber [39, 140, 141], soy protein isolate [38], poly(vinyl alcohol) [42, 44], chitosan [41, 141], silk fibroin, [142], alginate [44], starch [143], hyaluronan–gelatin [55], and waterborne polyurethane [144, 145].

2. *Freeze-drying and hot-pressing technique*

Another method called freeze-drying and hot-pressing has also been used to prepare polymer/CW nanocomposites [37, 39, 40]. In this method, the blends of polymer and CW were also prepared in water medium to get well-dispersed aqueous mixtures, which were then freeze-dried to give nanocomposite powders, and the powders were consequently processed into specimen by hot-pressing. This method can be used only when a thermoplastic polymer is used as the matrix. If those polymers which would undergo crosslinking or have lower decomposition temperature than their melting temperature were used as the matrix polymers, their CW based nanocomposites cannot be prepared by this method since they are unable to be hot-pressed. Such polymers include waterborne polyurethane [144], vulcanized rubber [39, 141], chitosan [41, 141], and poly(vinyl alcohol) [42]. Their CW filled nanocomposites were predominantly prepared by casting and evaporating method. Polymer/CW nanocomposites produced by the two techniques usually showed different physical properties due to the different morphology of the composite and the fact that different interactions between whiskers can establish [37, 39, 141]. The distribution morphologies of CW in polymer matrix may be different for the composites obtained by casting and evaporating and freeze-drying and hot-pressing methods although aqueous mediums were used for the two techniques. The cryo-fractured surfaces for unvulcanized natural rubber/CW nanocomposties prepared by the two methods were comparatively observed by SEM as reported by Nair et al. [39] The SEM micrographs are shown in Fig. 3.27. In Fig. 3.27a, the CWs appear as white dots, which are distributed evenly throughout the evaporated unvulcanized natural rubber matrix.

It seems there is no significant difference between Figs. 3.27a (casted and evaporated film) and 3.27b (freeze-dried and hot-pressed film), however, there are broader smooth unfilled regions in Fig. 3.27b, which is an indication of poorer whisker distribution in freeze-dried and hot-pressed composites. The reason for the relatively poorer distribution might be ascribed to the self aggregation of CW during hot-pressing. So, casting-evaporating technique is a more effective way to prepare well-dispersed CW nanocomposites.

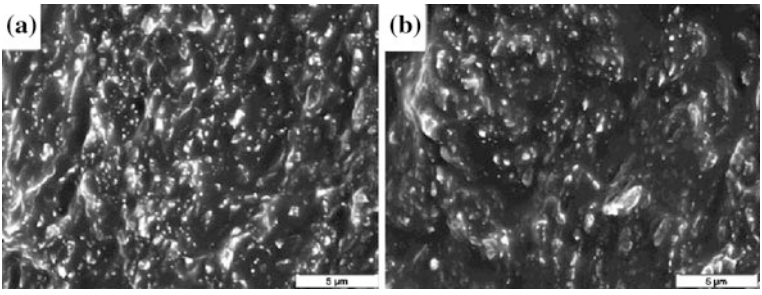


**Fig. 3.27** Scanning electron micrographs of the cryo-fractured surfaces of unvulcanized natural rubber/CW obtained by casting and evaporating (**a**) and freeze-drying and hot-pressing (**b**) [39]

3. *Polymer grafting*

A solvent free technique, "graft from" strategy, was reported to prepare chitin whisker-graft polycaprolactone (CW-g-PCL) nanocomposites [146] CW powders were first obtained by lyophilization of CWs suspension. The CW-g-PCL nanocomposites were prepared by bulk ring-opening polymerization of caprolactone in the presence of CWs of which the surface hydroxyl groups work as initiation sites. The resulting products can be shaped by thermoforming. The shortcoming of this technique is that the amount of CWs is limited (less than 2 wt%) since high-molecular-weight PCL is unobtainable when the content of CWs is too high. Thus, strong reinforcement may not be anticipated with such small content of CWs.

4. *Non-aqueous solvent dispersion technique*

Same as other traditional nanoparticles, polysaccharide nanocrystals are also easy to self-aggregate and even form the agglomerates in micrometer scale. The self-aggregation reduces positive function of nanocrystals in nanocomposites [146]. There are a large number of hydroxyl groups on the surface of the polysaccharide nanocrystals, which make them hydrophilic. These hydroxyl groups endow two characteristics with polysaccharide nanocrystals. On one hand, they make polysaccharide nanocrystals thermodynamically immiscible with most of hydrophobic polymers; thus, it is difficult to achieve well dispersed nanocomposites through simple melt compounding of hydrophobic polymers with polysaccharide nanocrystals. PCL/CW nanocomposites were reported to be processed by melt compounding of poly(caprolactone) and freeze-dried CW, however, the morphology of the nanocomposite has not been shown thus the dispersion of whiskers in the polymer matrix cannot be evaluated [4]. On the other hand, these hydroxyl groups are very reactive thus make their modification very easy by various surface chemical reactions which are able to improve the hydrophobicity of polysaccharide nanocrystals [147, 148]. With improved hydrophobicity, these nanocrystals can disperse in non-aqueous solvents and be more compatible with hydrophobic polymers [149]. Therefore, melt compounding and non-aqueous solution mixing techniques are possible for preparing well dispersed polymer/polysaccharide nanocrystals reinforced nanocomposites. After surface hydrophobic modification, CWs can form a good dispersion in non-aqueous solvent, then, nanocomposites can be prepared in non-aqueous medium. The surface of crab shell CWs were chemically modified using different reactive compounds such as alkenyl succinic anhydride (ASA), phyenyl isocyanate (PI), and isopropenyl-α, α'-dimethylbenzyl (TMI). Figure 3.28 shows TEM images of CWs before and after modification. After surface chemical modification with ASA and PI, the appearance of the chitin fragments changed to be entangled, and individual whiskers were difficult to observe. The surface modified CWs can disperse in toluene and form stable dispersion, whereas, unmodified CWs cannot disperse in toluene. The natural rubber/CWs nanocomposites were prepared using toluene as a medium. The removal of toluene resulted in nanocomposites films in which CWs and natural rubber matrix showed improved adhesion [141].

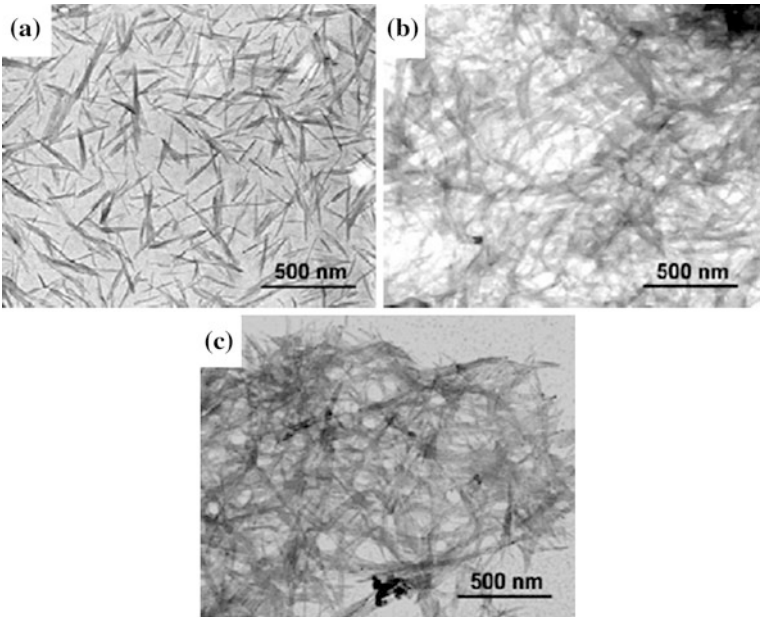


**Fig. 3.28** Transmission electron micrographs of a dilute suspension of **a** unmodified, **b** ASA modified, and **c** PI-modified chitin whiskers [141]

5. *Extrusion and impregnation*

Very few studies have been reported concerning the processing of polysaccharide nanocrystal-reinforced nanocomposites by extrusion methods. The hydrophilic nature of polysaccharides causes irreversible agglomeration during drying and aggregation in non-polar matrices because of the formation of additional hydrogen bonds between amorphous parts of the nanoparticles. Therefore, the preparation of cellulose whiskers reinforced poly lactic acid (PLA) nanocomposites by melt extrusion was carried out by pumping the suspension of nanocrystals into the polymer melt during the extrusion process [150]. An attempt to use PVA as a compatibilizer for promoting the dispersion of cellulose whiskers within the PLA matrix was reported [151]. Organic acid chlorides-grafted cellulose whiskers were extruded with LDPE [152]. The homogeneity of the ensuing nanocomposite was found to increase with the length of the grafted chains.

An attempt to use a recently patented concept (Dispersed Nano-Objects Protective Encapsulation—DOPE process) intended to disperse carbon nanotubes in polymeric matrices was reported. Physically cross-linked alginate capsules were successfully formed in the presence of either cellulose whiskers or microfibrillated cellulose [153]. The resulting capsules were extruded with a thermoplastic material. Another possible processing technique of nanocomposites using cellulosic nanoparticles in the dry state present in the filtration of the aqueous suspension to obtain a film or dried mat of particles followed by immersion in a

polymer solution. The impregnation of the dried mat was performed under vacuum. Composites were processed by filling the cavities with transparent thermosetting resins such as phenol formaldehyde [154, 155], epoxy 178], acrylic [155–158] and melamine formaldehyde [159].

Nonwoven mats of cellulose microfibrils were also used to prepare polyurethane composite materials via film stacking method [160]. Water-redispersible nanofibrillated cellulose in powder form was recently prepared from refined bleached beech pulp by carboxymethylation and mechanical disintegration [161]. However, the carboxymethylated sample displayed a loss of crystallinity and strong decrease in thermal stability limiting its use for nanocomposite processing.

6. *Electrospinning*

Electrostatic fiber spinning or "electrospinning" is a versatile method to prepare fibers with diameters ranging from several microns down to below 100 nm through the action of electrostatic forces. It uses an electrical charge to draw a positively charged polymer solution from an orifice to a collector. Electrospinning shares characteristics of both electrospraying and conventional solution dry spinning of fibers. The process is non-invasive and does not require the use of coagulation chemistry or high temperatures to produce solid threads from solution. This makes the process particularly suited for the production of fibres using large and complex molecules. Bacterial cellulose whiskers were incorporated into POE nanofibers with a diameter of less than 1 μm by the electrospining process to enhance the mechanical properties of the electrospun fibers [162]. The whiskers were found to be globally well embedded and aligned inside the fibers, even though they were partially aggregated. Electrospun polystyrene (PS) [163], PCL [164] and PVA [165] microfibers reinforced with cellulose nanocrystals were obtained by electrospinning. Nonionic surfactant sorbitan monostearate was used to improve the dispersion of the particles in the hydrophobic PS matrix.

7. *Multilayer films*

The layer-by-layer assembly (LBL) is a method by which thin films particularly of oppositely charged layers are deposited. Thin film LBL assembly technique can also be utilized for nanoparticles. In general the LBL assembly is described as sequential adsorption of positive or negative charged species by alternatively dipping into the solutions. The excess or remaining solution after each adsorption step is rinsed with solvent and thus a thin layer of charged species on the surface ready for next adsorption step is obtained. There are many advantages of the LBL assembly technique and these include simplicity, universality and thickness control in nanoscale. Further the LBL assembly process does not require highly pure components and sophisticated hardware. For almost all-aqueous dispersion of even high molecular weight species, it is easy to find an LBL pair that can be useful for building thin layer. In each adsorption step, either a monolayer or a sub monolayer of the species is obtained and, therefore the number of adsorption steps needed for a particular nanoscale layer can be determined. The use of the LBL technique is expected to maximize the interaction between cellulose whiskers and a polar

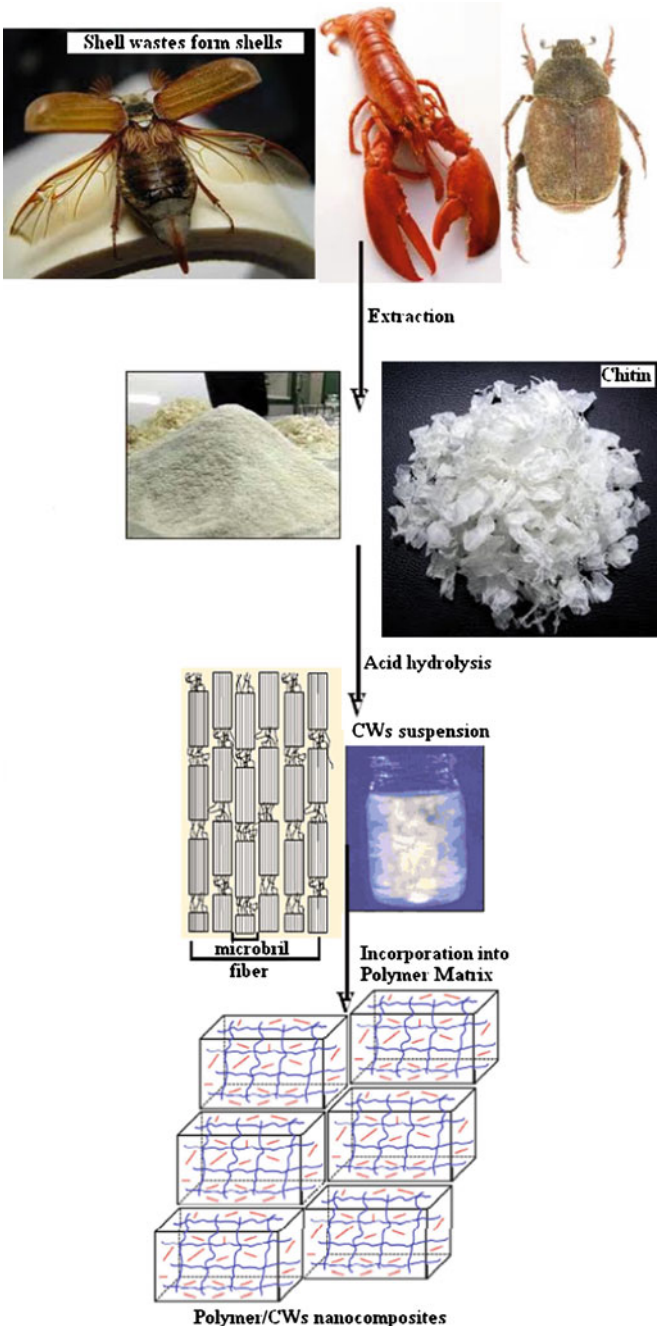


**Fig. 3.29** Synthetic routes for the synthesis of polymer/chitin nanocomposites

polymeric matrix, such as chitosan [166]. It also allows the incorporation of high amounts of cellulose whiskers, presenting a dense and homogeneous distribution in each layer. Podsiadlo et al. [167] reported the preparation of cellulose whiskers multilayer composites with a polycation, poly-(dimethyldiallylammonium chloride) (PDDA), using the LBL technique. The authors concluded that the multilayer films presented high uniformity and dense packing of nanocrystals.

Orientated self-assembled films were also prepared using a strong magnetic film [168] or spin coating technique [169]. The preparation of thin films composed of alternating layers of orientated rigid cellulose whiskers and flexible polycation chains was reported [170]. Alignment of the rod-like nanocrystals was achieved using anisotropic suspensions of cellulose whiskers. Green composites based on cellulose nanocrystals/xyloglucan multilayers have been prepared using the non-electrostatic cellulose-hemicellulose interaction [171]. The thin films were characterized using neutron reflectivity experiments and AFM observations. More recently, biodegradable nanocomposites were obtained from LBL technique using highly deacetylated chitosan and cellulose whiskers [166]. Hydrogen bonds and electrostatic interactions between the negatively charged sulfate groups on the surface of nanoparticles and the ammonium groups of chitosan were the driving forces for the growth of the multilayered films. A high density and homogeneous distribution of cellulose nanocrystals adsorbed on each chitosan layer, each bilayer being around 7 nm thick, were reported. Self-organized films were also obtained using only charge-stabilized dispersions of celluloses nanoparticles with opposite charges [172] from the LBL technique.

The overall processing for the polymer chitin whiskers nanocomposites is outlined in Fig. 3.29.

## 3.7 Characterization of Chitin Nanocomposites and Blends

The properties of high performance chitin filled natural rubber (NR) nanocomposites were carefully analyzed by Gopalan et al. [72]. It was concluded that the whiskers form a rigid network in the NR matrix which is assumed to be governed by a percolation mechanism. A percolated filler–filler net work is formed by hydrogen bonding interaction between chitin particles above the percolation threshold. The values of diffusion coefficient, bound rubber content, and relative weight loss also supported the presence of a three-dimensional chitin network within the NR matrix. The mechanical behavior of the composites gives additional insight and evidence for this fact. Rujiravanit and coworkers [42] studied thermal stability of the chitin nanocomposites by TGA. The presence of the whiskers did not affect much the thermal stability and the apparent degree of crystallinity of the chitosan matrix. The tensile strength of α-chitin whisker-reinforced chitosan films increased from that of the pure chitosan film with initial increase in the whisker content to reach a maximum at the whisker content of 2.96 wt% and decreased gradually with further increase in the whisker content, while the percentage of

elongation at break decreased from that of the pure chitosan with initial increase in the whisker content and leveled off when the whisker content was greater than or equal to 2.96 wt %. The crystallinity of the PVA/chitin nanocomposites; the presence of the whiskers did not have any effect on the crystallinity of the PVA matrix [42]. They suggested that the cast PVA film was essentially amorphous for the α-chitin whiskers, their WAXD pattern exhibits two major scattering peaks at $2\theta$ angles of about 9 and 19°, respectively, for the resulting α-chitin whisker reinforced PVA films. The WAXD patterns were intermediate to those of the pure components with the strong scattering peaks of α-chitin whiskers (i.e. at about 9 and 19°) being more pronounced with increasing whisker content. To verify whether or not incorporation of α-chitin whiskers into PVA resulted in an increase in the crystallinity of the PVA matrix, FT-IR spectra were considered. The peak at 1144 $cm^{-1}$ (C–O of doubly H-bonded OH in crystalline regions) was useful for indication of the crystallinity of PVA. Apparently, the relative intensity of this peak was not found to increase with increasing whisker content, indicating that incorporation of α-chitin whiskers did not have an effect on the crystallinity of the PVA matrix. Lu et al. [38] described that the chitin filled SPI composites showed an increase in Young's modulus and tensile strength from 26 to 158 MPa and 3.3 to 8.4 MPa with increasing chitin contents from 0 to 20 wt%. As the chitin whiskers increase in the SPI matrix, the composites showed greater water-resistance. The improvement in all of the properties of these novel SPI/chitin whisker nanocomposites may be ascribed to three-dimensional networks of intermolecular hydrogen bonding interactions between filler and filler and between filler and SPI matrix. Spriupayo and co-workers [42] have determined the TGA thermograms of pure PVA, α-chitin whiskers, and α-chitin whisker-reinforced PVA nanocomposites films having whisker content of 14.8 and 29.6 wt %, respectively. All of the samples showed initial weight loss at about 60–80 °C, due to the loss of moisture upon heating. The moisture content in these samples was almost similar (i.e. about 8 %). According to the derivative TGA curves, pure PVA film exhibited a major degradation peak at 274 °C while as prepared α-chitin whiskers showed a major degradation peak at 347 °C curve (d)). The major degradation peaks for PVA films reinforced with 14.8 and 29.6 wt% α-chitin whiskers were intermediate to those of the pure components, with the thermal stability of the nanocomposite films increased with increasing α-chitin whisker content.

In another study, the bare and enzyme immobilized $SiO_2$-chitin/CNTs bio-nanocomposite was characterized with Fourier transform infrared spectroscopy (FTIR), scanning electron microscopy (SEM) and cyclic voltammetry (CV). In the FTIR spectra, the infrared peaks of chitin in $SiO_2$-chitin become wider and sharper due to overlap of functional groups of chitin and $SiO_2$, i.e., stretching vibration bands of Si–O–Si, Si–O–C and C–O bond. In addition, two new peaks appear at 1,300 and 785 $cm^{-1}$ pertaining to stretching vibration of C–Si and bending vibration of C–H corresponding to $CH_3$-Si group [173]. On incorporation of CNTs in CH-$SiO_2$ hybrid, the infrared band corresponding to $SiO_2$ becomes broader and a new infrared band appears at 890 $cm^{-1}$ revealing presence of CNTs that affects vibration mode of chitin and $SiO_2$ resulting in the formation of $SiO_2$-chitin/CNTs

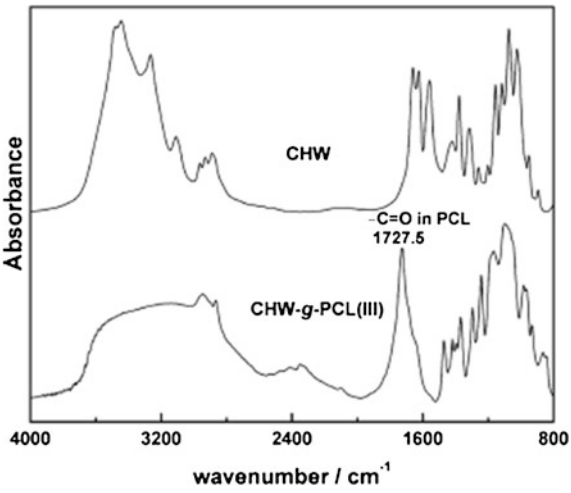


**Fig. 3.30** FTIR spectra of the CW and CW-g-PCL(III) powders, where the CW-g-PCL(III) is used as the representative of grafted CW [174]

bio- nanocomposite. After immobilization of enzyme, FTIR bands corresponding to -NH/-OH group in nanobiocomposite become broader suggesting interaction between amino and hydroxyl group of chitin. However, presence of peaks at 1,672 and 1,442 $cm^{-1}$ (corresponding to amide bands) indicates immobilization of enzymes. The surface morphology of $SiO_2$-chitin/CNTs reveals the monodispersed rope like structure of CNTs surrounded with globular appearance of $SiO_2$ particles into chitin matrix indicating that CNTs and $SiO_2$ are uniformly dispersed into the backbone of chitin. So it can be speculated that CNTs are rapped with chitin and $SiO_2$ via electrostatic interactions. The surface morphology of $SiO_2$-chitin/CNTs nanobiocomposite further changes after the immobilization of enzyme revealing attachment of enzymes over the electrode surface. Feng et al. [174] reported the structure and properties of new thermoforming bionanocomposites based on chitin whisker-graft-polycaprolactone (chitin-g-PCL).

FTIR spectra of the chitin-g-PCL(III) and chitin powders are depicted in Fig. 3.30. The spectrum of pure chitin was compared with that of spectrum of-chitin-g-PCL, the prominent change observed after grafting process was the appearance of one distinct peak located at 1727.5 $cm^{-1}$ assigned to ester-carbonyl group of grafted PCL chains. It indicated that the PCL and chitin were successfully linked together. The SEM and TEM images of CW and CW-g-PCL(III) nano-particles are presented in Figs. 3.31 and 3.32 respectively.

Ramaprasad et al. [89] synthesized the chitin-polyaniline nanocomposite by electron beam irradiation method. UV–Vis spectra showed the decrease in the intensity of peak at 630 nm due to formation of low-energy electron beam *(*LEB*)* during irradiation. IR analysis showed the interaction between chitin and PANI. SEM micrograph showed the formation of chitin-PANI nanocomposite. XRD analysis confirmed the formation PANI particles in the blend solution.

Electrical study showed the increase in the conductivity due to irradiation up to certain level and then conductivity decreases. TGA analysis showed that blends

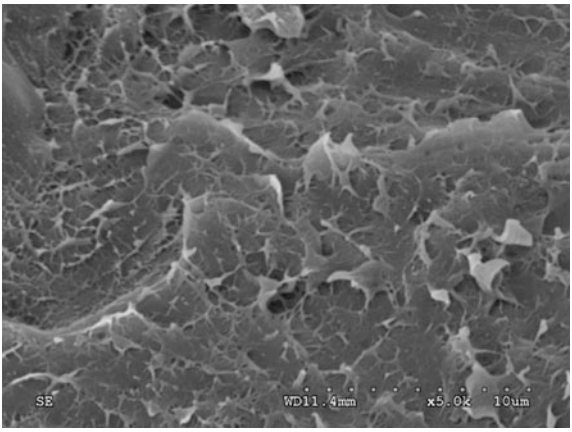


**Fig. 3.31** SEM image of fractured surface for the thermoforming CW-g-PCL(III) sheet as the representative of all the sheets [174]

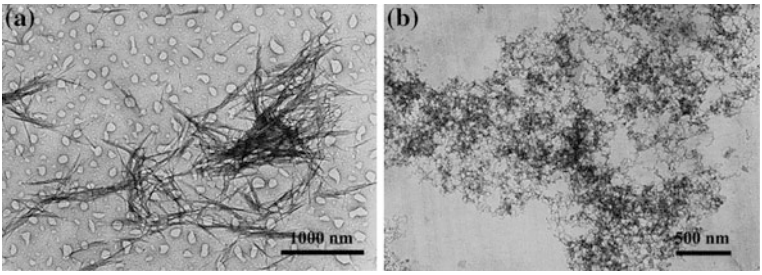


**Fig. 3.32** TEM images of the CW and CW-g-PCL(III) nanoparticles, where the CW-g-PCL(III) is used as the representative of grafted CW [174]

are more stable after irradiation. Finally, the formation of PANI particle during irradiation in the blend solution is due to the presence of chitin, where as no particle formation is observed in pure PANI solution irradiated with electron beam. The detailed presentation of effect of radiation on chitin and PANI is presented in Fig. 3.33.

Zia et al. [115] presented that nanostructure and morphological pattern of chitin/bentonite clay based polyurethane bionanocomposites. The clay dispersion within chitin was characterized by both XRD and optical microscopy (OM), which is the most frequently, used and approachable methods to study the structure of nanocomposites. There are one acetamide ($-NHCOCH_3$) group at C-2 position and two (two hydroxy (–OH)) groups at C-3 (C3–OH) and C-6 (C6–OH) positions on chitin chains which can serve as the coordination and reaction sites [95]. The crystalline structure of chitin has been reported by many researchers [96].

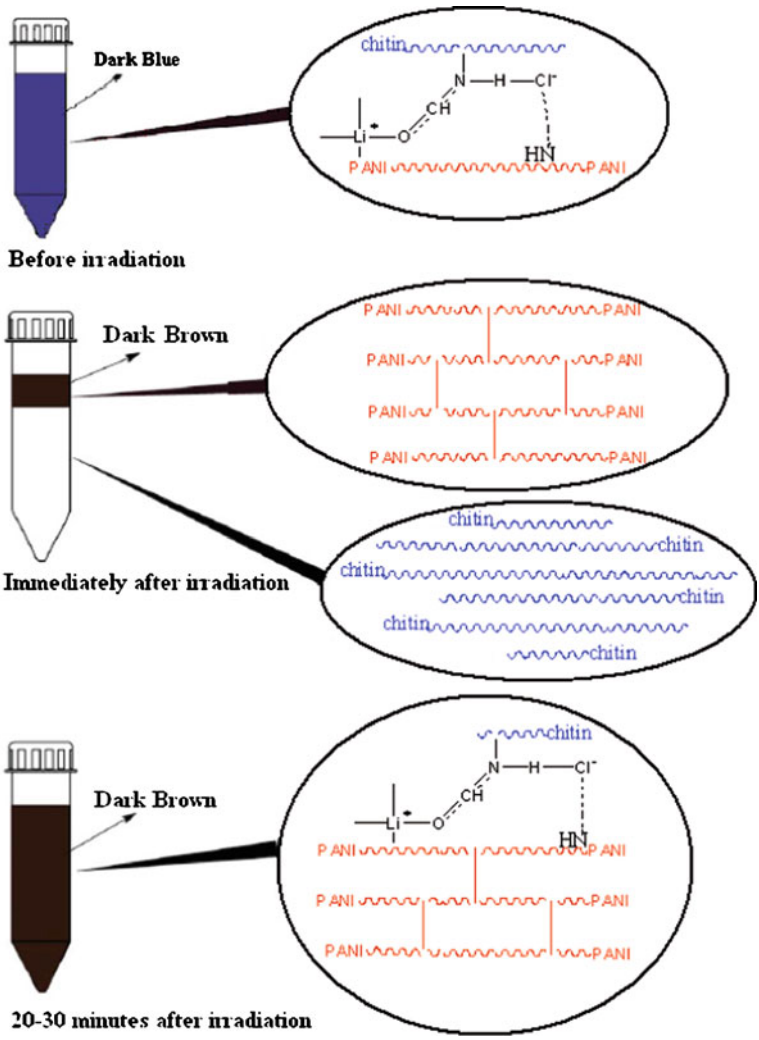


**Fig. 3.33** Effect of radiation onto chitin and polyaniline [89]

## *3.7.1 Properties of Polymer/CW Nanocomposites*

1. *Mechanical properties*

Tensile testing of single crystalline metallic microwhiskers can also be studied following the experimental tensile testing constructed by Brenner and (b) results of whisker fracture strength as a function of whisker size, showed the clear size dependence (Fig. 3.34). The chitin whiskers are usually incorporated into polymer matrix to prepare CWs reinforced polymer nanocomposite. Thus, the mechanical

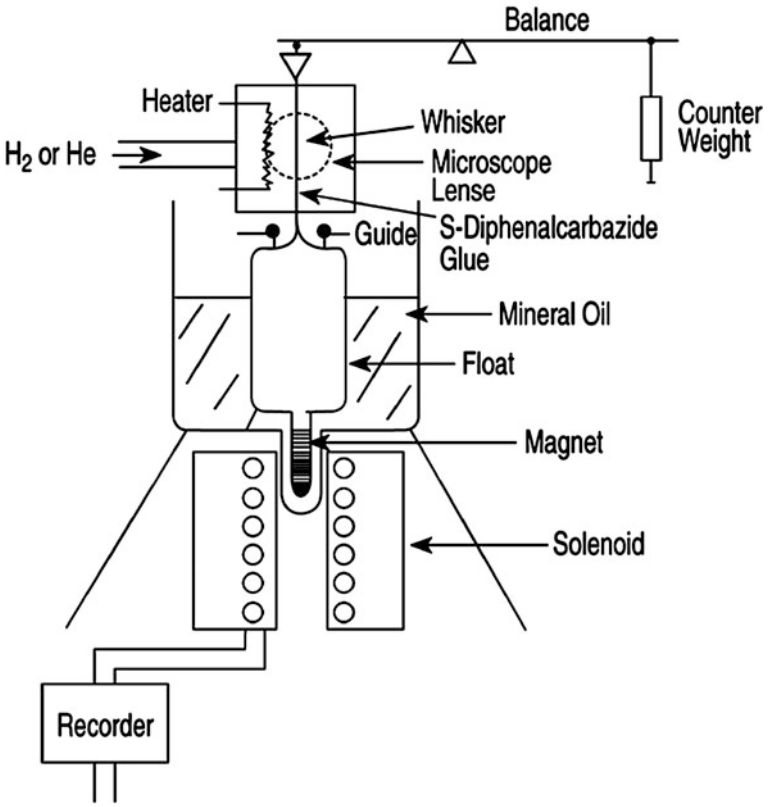


**Fig. 3.34** Tensile testing of single crystalline metallic microwhiskers [175]

properties are of the first importance for CW reinforced nanocomposites. The improvement in mechanical properties especially modulus has been achieved in many polymer/CW systems. There are several factors which affect the reinforcing effect of polymer/CW nanocomposites, including the glass transition temperature of polymer matrix, the aspect ratio (L/D ratio) of CWs, the loading of CW, and nanocomposite processing techniques. Taking poly(S-*co*-BuA)/CW system for an example [175], at temperature range lower than *T*g of poly(S-*co*-BuA), the increase in storage shear modulus was very limited with CW obtained from squid pen chitin introduced or increased; however, when the temperature increased to higher than *T*g of poly(S-*co*-BuA), the relaxed modulus of the nanocomposites increased significantly when the loading of CW was more than 10 wt%, and more than 25 and 160 times improvement in modulus were achieved when CW loadings were 10 and 20 wt% at $\sim$300 K (*T*g + 25 °C), respectively. It was found that when CW loading was less than 5 wt%, almost no reinforcement occurred for poly(S-*co*-BuA)/CW nanocomposite. The reinforcing effect of the CW is much less pronounced than the one observed for tunicin whisker filled composites.

The differences in reinforcing effect of the two kinds of whiskers are ascribed to their different aspect ratios.

The reinforcing effect strongly depends on the aspect ratio of nanocrystals, and higher aspect ratio usually brings about greater reinforcement as been proved in comparative study of starch and cellulose nanocrystals [176]. The aspect ratio for tunicin whisker is around 50–200 [19], but that of squid pen chitin whisker is only about 15. When riftia tubes CWs with aspect ratio of 120 was used as nanofillers for poly(S-*co*-BuA), a significant modulus increase was observed even with only 1 wt% whisker loading [37]. The effects of processing methods on the mechanical properties of natural rubber/crab shell CW nanocomposites were investigated in detail by Nair et al. [39, 140]. The nanocomposites with unvulcanized natural rubber as the polymer matrix were prepared by two techniques, freeze-drying and hot-pressing method and casting and evaporating method. The samples prepared by casting and evaporating method showed higher reinforcing efficiency than those prepared by freeze-drying and hot-pressing method. It is believed that a three-dimensional CWs network was formed driving by the strong hydrogen bonding during evaporation method, as been proved by swelling behavior of composite films. The three dimensional network of cellulose whiskers was also reported to be formed during preparation of poly(S*co*-BuA)/CW and Mcl-PHA/CW nanocomposites by evaporation methods [17, 33]. The tensile properties of polymer matrix could be changed greatly by incorporation of CWs. Generally speaking, the tensile strength and Young's modulus could be improved at the cost of ductility. The CW loading plays an important role in the improvement of tensile properties of the nanocomposites. The optimum loadings are various for different polymer matrices and CW origins and usually less than 5 wt% since CW tends to aggregate with higher CW content, which will lead to negative effects on the mechanical properties. For poly (vinyl alcohol)/CW and chitosan/CW nanocomposites, the highest tensile strength was obtained with CW loading at 2.96 wt% [41, 42]. The maximum tensile strength for glycerol plasticized-potato starch (GPS)/CW [143] waterborne polyurethane/CW [145] and hyaluronan–gelatin/CW [55] nanocomposites happened at the CW loading of 5, 3, and 2 wt%, respectively. The elongation at break of all the related nanocomposites gradually decreased with increase of CW loading. CWs were also reported to reinforce polymer nanocomposites/nanofibers. The polymer/CW nanocomposites nanofibers are prepared by electrospinning or wet spinning of mixture of water soluble polymer aqueous solution and CW suspension. PVA/CW nanocomposite fiber mats with different amounts of CW were prepared by electronspinning, and the Young's modulus of the nanocomposite fiber mat was 4–8 times higher than that of neat PVA fiber mat. The storage modulus of PVA nanofiber mat increased with CW loading in the considered range. Alginate/CW nanocomposite fibers with 0.5–2.0 wt% CW were prepared by wet spinning. The incorporation of such low amount of CW in the nanocomposite fibers improved the mechanical properties significantly due to possible specific interactions, i.e., hydrogen bonding and electrostatic interactions, between the alginate molecules and the homogeneously dispersed CWs [44]. The surface modification of CW could also affect the mechanical properties of

polymer/CW nanocomposites. The crab shell CW was reported to be treated with PI, ASA and TMI separately and then incorporated into natural rubber matrix. The interactions between natural rubber matrix and CW increased by the surface treatment of CW, however, rubber/modified CW showed poorer mechanical properties compared to rubber/unmodified CW composites. The poorer reinforcing effect may be ascribed to lack of formation of whisker network after surface modification which would reduce the driving force of network formation and hydrogen bonding [141].

On the basis of the influence factors of reinforcing efficiency when using CW as reinforcing filler, we can conclude that high reinforcing effects are easier to be obtained when low *T*g polymers such as natural rubber and polycaprolactone were used as matrixes and that the reinforcing efficiency increased with aspect ratio of CW, which were similar to other nanocomposites consisting of polymer and inorganic nanofillers [177]. Although surface hydrophobic modification of CW could improve compatibility with polymers, the reinforcing effect could not be simultaneously improved since whisker network is difficult to be formed after surface modification.

2. *Swelling behavior*

The interaction of polymeric materials with solvents is a problem from technological points of view, since the dimensions and physical properties of materials may be changed due to the penetration of solvents into specimens. A rigid cellulose network can be formed within polymer matrix by three-dimensional hydrogen bonding between cellulose whiskers during the films formation, which is very helpful for hindering diffusion of solvent in the polymer matrix, thus improve solvent resistance of polymer/CW nanocomposites. Although the hydrogen bonding of chitin is somewhat weaker than cellulose, a similar rigid network can also be formed during the preparation of polymer/CW nanocomposites by casting-evaporation method. The swelling of vulcanized natural rubber/chitin whisker (PCH) nanocomposites, prepared by casting-evaporation, in toluene were investigated by Dufresne et al [39]. The toluene uptake of the PCH nanocomposites is rapid in the initial zone ($t < 5$ h), afterwards, the sorption rate decreases leading to a plateau, corresponding to equilibrium absorption. The equilibrium toluene uptake value of neat vulcanized natural rubber was 488 %, which gradually decreases to 413, 331, 282, and 239 % for the PCH nanocomposites with CW loading of 5, 10, 15 and 20 % respectively. The diffusion coefficient of toluene gradually decreases with increasing the loading of CW, down to $4.4 \times 10^{-8}$ $cm^2$ $s^{-1}$ for 20 % loading. The results were ascribed to the increased stiffness of chitin network and interactions between VNR and CW with increase of CW loading. Water resistance of hydrophilic polymers can also be improved by incorporation of CW to form nanocomposites. The water swelling of glycerol plasticized soy protein isolate/chitin whiskers (SPI/CW) nanocomposites was investigated by Lu et al. [38]. The water uptake SPI sheet was about 40 %, whereas that of the SPI/chitin nanocomposites decreases with increasing CW content, e.g., only about 23 % for SPI-30 composite, suggesting an improvement of water resistance. The

diffusion coefficient of water in SPI/CW nanocomposites was much lower than in SPI sheet. The results were also attributed to the formation of stronger chitin network with increase of CW content. The water absorption of other CW filled nanocomposites such as PVA/CW [42] and CS/CW [41] was also studied and similar results were obtained with incorporation and increasing loading of CW.

3. *Barrier properties*

Barrier properties increase shelf life period by protecting the inside product from deteriorations through oxidation, humidity or bacteria [16]. Polymer nanocomposites with well-dispersed nano-clay showed improved barrier properties compared with the neat polymer matrix. Starch nanocrystal showing platelet morphology similar to clay nanosheet can improve barrier properties of polymer matrix by forming nanocomposites [16, 178, 179]. Although cellulose whisker shows rodlike morphology, the improvement in barrier properties was also observed for polymer/CW nanocomposite [49, 180]. CW possesses similar morphology to cellulose whisker. The barrier properties of polymer/CW nanocomposites have not been investigated widely. Only Chang et al. [143] investigated the water vapor permeability (WVP) of glycerol plasticized starch/chitin nanoparticle (GPS/CNP) composites. WVP of GPS reached a peak value when the CNP content increased from 1 to 3 w %. The improvement in water vapor barrier by incorporation CNP was ascribed to the tortuous path for water molecules to pass through the composites [181].

4. *Thermal properties*

It has been reported that the glass transition temperature ($T$g) of host polymers seems independent of CW concentration [37]; however, the $T$g value of the host polymer was usually lower than those of their CW nanocomposites prepared by casting-evaporation technique [37, 145]. The increased $T$g was ascribed to the fact that the existence of high specific area of CW in the composites would restrict the molecular mobility of polymer chains. For CW-g-PCL copolymer nanocomposites, the α-relaxation temperature determined by DMA gradually increased with increase of CW concentration, indicating that the segment mobility of PCL gradually decreased with CW concentration [146]. The melting point temperature ($T$m) was also reported to be independent of the CW concentration for PCL/CW nanocomposites; however, the enthalpic changes at melting transition ($\Delta H$m) and the deduced degree of crystallinity ($x$c) of PCL in nanocomposites were systemically lower than those of neat PCL, which might be due to the fact that CWs might slow down the crystallization kinetics of PCL [37, 40]. Nevertheless, the $T$m and $\Delta H$m of CW-g-PCL copolymer nanocomposites almost keep unchanged with CW concentration in the range of 1 ∼1.42 wt% has been reported by Feng [146]. The thermal stability of polymer/CW nanocomposites has been investigated occasionally. Most studies suggested that incorporation of CWs into polymer matrix improves thermal stability of the matrix very slightly especially when the content of CW was less than 10 % [41, 42, 55]. Some published references indicated that the onset decomposition temperature gradually increased with CW

content [40]. Limited researches demonstrated that the quite visible distinct increase in thermal stability could be achieved when the content of CW was high enough, for example 30 wt%, the improvement in thermal stability was ascribed to the increased matrix-CW interaction and the formed CW network with increase of CW content [144].

5. *Other properties*

Because of the reinforcing effect, CWs were incorporated into some potential biomedical materials, such as hydrogels and scaffolds, in which the materials have to possess non-cytotoxicity. When CW was incorporated into silk fibroin to form reinforced nanocomposite sponges, it not only improved the dimensional stability but also promote the cell spreading on the nanocomposite materials [142]. Zhang et al. [182] introduced three different polysaccharide nanocrystals into cyclodextrin/polymer inclusion supramolecular hydrogels to enhance mechanical strength and regulate drug release behavior of the hydrogels, and the in vitro cell viability of the extracted leached media from the nanocomposite and native hydrogels was evaluated by the MTT Cell *Proliferation* Assay using the L929 cell line. The results showed that incorporation of chitin whisker as well as cellulose and starch nanocrystals did not increase the cytotoxicity of the nanocomposite materials since they showed similar cell viability with native hydrogel. Hariraksapitak et al. [55] incorporated CW into hyaluronan–gelatin to manufacture reinforced nanocomposite scaffolds and investigated their cytotoxicity. The results suggested that with 10 wt% CW incorporated in the nanocomposite scaffold showed the greatest cell viability even higher than native scaffold. All the results suggested that CW is non-toxic and can be used in biomedical materials. One of the advantages of polysaccharide nanocrystals over inorganic nanofiller in reinforcing polymer nanocomposites is their biodegradability, which makes them very competitive particularly in reinforcing biodegradable thermoplastics since fully biodegradable nanocomposites can be produced. Watthanaphanit et al. [44] incorporated CW into alginate to produce reinforced nanocomposite fibers by wet spinning process. The biodegradation of the nanocomposite fibers was investigated in Tris–HCl buffer solution containing lysozyme and the results suggested that the addition of the CWs in the nanocomposite fibers could accelerate the biodegradation process.

## 3.8 Applications of Chitin and Their Nanocomposites and Blendes

### *3.8.1 Applications of Chitin Whicker and Chitosan Nano-Fibers*

The blood compatibility of chitin and chitosan remains a prime aspect almost 20 years after Hirano reported his studies on chitosan and its acyl derivatives in 1985 [183]. A resurgence of these initial studies was reported by Lee et al. [184]

who confirmed the blood compatibility properties of N-acylchitosans. An N-acylation of 20–50 % was achieved and their susceptibility to lysozyme degradation was found to be comparable to acetyl-chitosan. Recent reports by Hirano et al. [185] concentrate on the production of chitosan collagen fibers that again were chemically modified and evaluated for their blood compatibility. The chitosan fiber was improved when collagen was added to chitosan as well as when the resultant chitosan-collagen fibers were N-derivatized. Anti-thrombogenic activity was obtained for collagen coated on N-acyl derivatized fibers similar to the results obtained in 1985. The chitosan fibers offer the potential of being fabricated into blood vessels and their blood compatibility results demonstrated in the recent work predicts well for applications where hemocompatibility is sought. Another noteworthy variation is the preparation of chitosan material that is subsequently chemically modified with an azide functionality to impart UV activation. Ishihara et al. [186] prepared a UV sensitive chitosan material that was crosslinked with lactose moieties to improve water solubility. The material, intended as a bioadhesive, was found to be non-cytotoxic and shown to have adhesive strength comparable to fibrin glue [187].

In order for chitin and chitosan to take their place as approved biomedical materials, two principal issues, biocompatibility and sterility, must be resolved [188]. These matters should be briefly discussed to reinforce their significance. Ikada and Tomihita [189] studied the degradation of chitin and chitosan films by lysozyme action and subcutaneous implant in a rat model. The rate of in vivo degradation was high for chitin reduction as the degree of deacetylation increased. Interestingly, the authors noted mild tissue reaction to chitosan. Similarly, Onishi and Machida [190] investigated the in vivo biodegradation of water-soluble chitosan using a mouse model. The approximately 50 % deacetylated material was found to be readily degraded and cleared by the animal suggesting no concerns in bioaccumulation. Other workers have looked at the effect of chitin and chitosan on biological systems. Tanaka et al. [191] found that when chitin and chitosan were administered orally or injected intra-peritoneally into a mice model, chitosan invoked a bigger reaction compared to chitin. Mori et al. [192] using cell culture assay, reported that chitin did not produce an acceleratory effect on L929 mouse fibroblasts proliferation. It was noted, however, that chitosan appeared to exhibit an inhibitory effect, attributing to the interaction of chitosan with growth factors thereby immobilizing the growth factors. This is in contrast to the report by Prasitsilp et al. [193] who found that a high degree of deacetylation in chitosan was more favorable for supporting cell growth, proliferation and attachment. This behavior was attributed to the electropositive nature of the amino group permitting interactions between chitosan and cells. It is clear that chitosan's effect on cell proliferation requires further study. Taking a different viewpoint, Fujinaga et al. [194] have chosen to study the effect of chitosan on wound healings. They found that chitosan accelerated the infiltration of polymorphonuclear (PMN) cells at the wound site. PMN also stimulated the production of osteopontin that promotes cell attachment, essential in tissue reorganization at the wound site. Okamoto et al. [195] found that chitin; neither chitosan nor glucosamine (chitosan monomer)

affected the proliferation of mouse 3T6 fetal fibroblasts or HUVEC (human umbilical vascular endothelial cells). However, the migration of cells, important during tissue reorganization, was affected by chitosan and glucosamine, warranting further study as to the effects of these biopolymers for wound healing applications. The authors suggest that further work should be performed to elucidate the mechanisms that chitin and chitosan invoke during wound healing [196]. Chitosan products intended for parenteral administration and those in contact with wounds will have to be sterilized before use. Common methods for the sterilization of pharmaceutical and medical products include exposure to dry heat, saturated steam, and ethylene oxide or $\gamma$ radiation. Before any of these methods are endorsed for the sterilization of chitosan products, their effects on the properties and end performance of the polymer will have to be documented.

Lim et al. [197] have been active in evaluating the effects of dry heat, saturated steam and $\gamma$-irradiation on chitosan based membranes. Ethylene oxide was not evaluated as it involves a chemical reactant that may be more reactive with chitosan to generate by-products and warranted a separate and specifically designed study. Exposure to dry heat resulted in lower aqueous solubility for chitosan and in extreme cases, insolubility in acidic aqueous media. This was found to be related to interchain crosslink formation involving the $NH_2$ groups in chitosan. A reduction of 60 % in tensile strength and 53 % reduction in the strain at break point were also experienced [198]. Saturated steam was also found to significantly accelerate the rate and extent of thermal events in chitosan. Chitosan became water insoluble and lost 80 % of its original tensile strength retaining only 28 % of the original strain at break point. The $\gamma$- irradiation caused main chain scission events in chitosan [199]. Chitosan membranes irradiated with 2.5 M-rad in air experienced a 58 % increase in tensile strength and a 22–33 % decrease in the swelling index of the membrane. Applying anoxic conditions during irradiation significantly reduced the changes to membrane properties. On the basis of these findings, it may be concluded that $\gamma$-irradiation at 2.5 M-rad under anoxic conditions provides the best means of sterilization for chitosan products. This study is in contrast to the findings by Rao and Sharma, [200] who recommended steam autoclaving although irradiation was not included in their study. The long-term storage effects have also to be thoroughly investigated as it will have implications on the integrity of chitin and chitosan materials [201]. Therefore, there remains a lot of scope to explore in the area of sterilization and storage before the method of sterilization and storage conditions can be optimized.

### *3.8.2 Applications of Chitin Nanocomposites and Blends*

New products are anticipated to be produced and the related physical properties for diverse applications need to be further investigated to take full advantage of the inexpensive and abundant annually occurring natural product, which coincides with sustainable development of human society. Recently, nano fibrous scaffolds

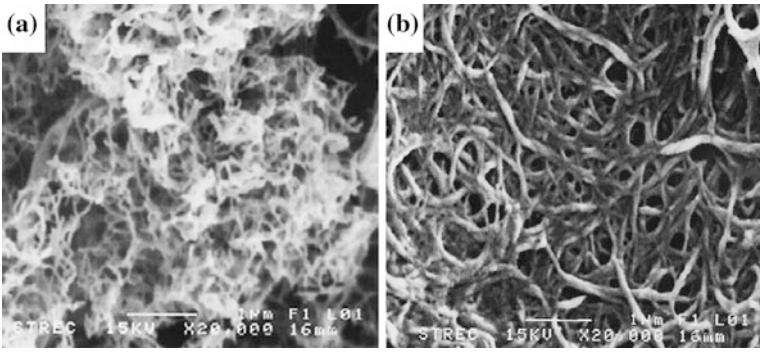


**Fig. 3.35** SEM micrographs of **a** chitin flakes (×20,000), **b** chitosan flakes (×20,000) [216]

based on chitin or chitosan have potential applications in tissue engineering. Tissue engineering is one of the most exciting interdisciplinary and multidisciplinary research areas today, and there has been exponential growth in the number of research publications in this area in recent years. It involves the use of living cells, manipulated through their extracellular environment or combined process to develop biological substitutes for implantation into the body and/or to foster remodeling of tissues in some active manners. It was reported that CWs can be used as raw materials to produce chitosan nanoscaffolds [202–204]. Phongying et al. [202] found that three times treatment of CWs by 40 % w/v NaOH aqueous solution at 150 °C for 7 h for each time would generate chitosan with degree of deacetylation of as high as 98 %. The micrographs from scanning electron microscope (SEM) and transmission electron microscope (TEM) confirm that the short fiber of CWs develop itself to be a network in nano-scale of chitosan or chitosan nanoscaffold by the alkali treatment. The aggregation and packing morphology of CW and morphology of chitosan nanoscaffolds are shown in Fig. 3.35. The chitosan nanoscaffolds showed porous structure with the pore diameter of ~200 nm. The produced nanoscaffolds are assumed to be nontoxic since the treatments were carried out in aqueous solution and the polymer matrix was natural polysaccharide, thus, are able to be used as tissue engineering materials. Because of non-toxicity, biocompatibility and biodegradability, CWs themselves or modified products have the potential to be used in many food and biomedical related areas.

Chitin nanofibers were found to promote cell attachment and spreading of normal human keratinocytes and fibroblasts compared to chitin microfibers [205]. This may be a consequence of the high surface area available for cell attachment due to their three-dimensional features and high surface area to volume ratios, which are favorable parameters for cell attachment, growth, and proliferation. The cell studies conducted on chitin/poly(glycolic acid) (chitin/PGA) [206] and chitin/silk fibroin (SF) [207] fibrous mats proved that a matrix consisting of 25 % PGA or SF and 75 % chitin had the best results. The chitin/PGA fibers had a bovine serum albumin coating and are considered as a good candidate for use in tissue-

engineering scaffold because normal human epidermal fibroblasts (NHEF) attached and spread. The chitin/SF fibrous mats had the highest spreading of NHEF and normal human epidermal keratinocytes (NHEK). Therefore, this scaffold is suggested for wound tissue engineering applications. Shalumon et al. [208] developed carboxymethyl cellulose/polyvinyl alcohol (CMC/PVA) blend nanofibrous scaffold for tissue engineering applications. The prepared nanofibers were bioactive and biocompatible. Cytotoxicity and cell attachment studies of the nanofibrous scaffold indicate that the nanofibrous CMC/PVA scaffolds can be safely used for tissue engineering applications. Bhattarai et al. [209] reported that the chitosan/polyethylene oxide (PEO) nanofibrous scaffolds promoted the attachment of human osteoblasts and chondrocytes and maintained characteristic cell morphology and viability throughout the period of study. This nanofibrous matrix is of particular interest in tissue engineering for controlled drug release and tissue remodeling. Similarly, Subramaniyan et al. [210] prepared chitosan/PEO nanofibers for cartilage tissue engineering. Cells were attached to the chitosan/PEO nanofiber mats slowly in the fist week. After 10 days, the more cells were attached on the surface of the nanofibers. These results indicated that the electrospun chitosan/PEO mats have been used for cartilage tissue repair. Mo et al. [211] also reported the smooth muscle cells attachment to the electrospun chitosan/collagen nanofibers after 30 days of culture.

The biological evaluations of chitosan/hydroxyapatite (HAp) nanfibrous composite scaffolds have been reported [212]. The chitosan/HAp nanofibrous scaffolds have significantly stimulated the bone forming ability as shown by the cell proliferation, mineral deposition, and morphology observation, due to the excellent osteoconductivity of HAp compared to the controlled chitosan. The results obtained from this study highlight the great potential of using the chitosan/HAp nanocomposite nanofibers for bone tissue engineering applications. A biocomposite of HAp with electrospun nanofibrous scaffolds was prepared by using chitosan/PVA and *N*-CECS/PVA for tissue engineering applications [213]. The cell studies showed that the L929 cell culture revealed the attachment and growth of mouse fibroblast on the surface of biocomposite scaffolds. Similarly, the potential use of the *N*-CECS/PVA electrospun fiber mats as scaffolding materials for skin regeneration was evaluated in vitro using L929 [214]. Indirect cytotoxicity assessment of the fiber mats indicated that the *N*-CECS/PVA electrospun mat was nontoxic to the L929 cell. Cell culture results showed that fibrous mats were good in promoting the cell attachment and proliferation. This novel electrospun matrix would be used as potential wound dressing for skin regeneration.

Liver tissue engineering requires a perfect extracellular matrix (ECM) for primary hepatocytes culture to maintain high level of liver-specific functions and desirable mechanical stability. Feng et al. [214] developed novel galactose/chitin (GC) nanofibers with surface galactose ligands to enhance the bioactivity and mechanical stability of primary hepatocytes in culture. The GC nanofibrous scaffolds displayed slow degradation and suitable mechanical properties as an ECM for hepatocytes according to the evaluation of disintegration and Young's modulus testing. The hepatocytes cultured on GC nanofibrous scaffold formed

stably immobilized 3D flat aggregates and exhibited superior cell bioactivity with higher levels of liver-specific function maintenance in terms of albumin secretion, urea synthesis and cytochrome P-450 enzyme than 3D spheroid aggregates formed on GC films. These results suggested that the GC-based nanofibrous scaffolds could be useful for various applications such as bioartificial liver-assist devices and tissue engineering for liver regeneration as primary hepatocytes culture substrates.

The plant and animal nanofibers (derived from waste and biomass) are uniformly mixed with resins and other polymers like plastics and rubbers to create natural based composite materials. A variety of plant fibers with high tensile strength can be used including kenaf, industrial hemp, flax, jute, sisal, coir etc. Fibers can be combined with traditional resins or newer plant based resins. The resulting component is a plant based alternative for many traditional steel and fiberglass applications. Advantages of bionanocomposites over traditional composites are reduced weight, increased flexibility, greater moldability, reduced cost, sound insulation and renewable nature. For environmental awareness and the international demand for green technology, nanobiocomposites have the potential to replace present petrochemical-based materials. They represent an important element of future waste disposal strategies. In true bionanocomposites, both the reinforcing material such as a natural fiber and the matrix are biodegradable. Cellulose, chitin and starch are the most abundant organic compounds in nature; they are also inexpensive, biodegradable, and renewable. They obviously receive a great attention for non-food applications. The use of natural fibers instead of traditional reinforcement materials, such as glass fibers, carbon, and talc, provides several advantages including low density, low cost, good specific mechanical properties, reduced tool wear, and biodegradability. These important applications include packaging, environment-friendly biodegradable composites, biomedical composites for drug/gene delivery, tissue engineering applications and cosmetic orthodontics. They often mimic the structures of the living materials involved in the process in addition to the strengthening properties of the matrix that was used but still providing biocompatibility, e.g. in creating scaffolds in bone tissue engineering.

## 3.9 Conclusion and Future Prospective

This chapter has demonstrated the utility of chitin and chitosan as potential materials for various implant applications and some of the challenges in demonstrating biocompatibility as well as sterility that must be addressed. The eventual realizations of real implants await the take-up of these materials on a more commercial basis that would see the introduction of chitin-based implantable devices. Chitin and its deacetylated derivative, chitosan, are non-toxic, biodegradable biopolymers currently being developed for use in biomedical applications such as tissue engineering scaffolds, wound dressings, separation membranes, antibacterial coatings, stent coatings, and sensors. Nano fibrous scaffolds based on chitin or chitosan have potential applications in tissue engineering. Electrospun

chitin and chitosan nano fibrous scaffolds would be used to produce tissue engineering scaffolds with improved cytocompatibility, which could mimic the native extracellular matrix (ECM). The preparation and tissue engineering applications of chitin and chitosan based nanofibers has also been summarized. Additional studies are necessary before clinical applications and for commercialization of the chitin and chitosan based nanofibers. This chapter will help to bring about newer innovative ideas for chitin andchitosan nanofibers for tissue engineering and other biomedical applications inthe future. Chitin and chitosan seem to be excellent dressing materials for the wound healing. The recent progress of chitin and chitosan-based fibrous materials, hydrogels, membranes, scaffolds and sponges in wound dressing has been overviewed. In the area of wound management, the use of chitin, chitosan and its derivative is immense.

As renewable and biodegradable nanoparticles, chitin whiskers are attracting and will continuously draw attention from both academic and industrial fields. Similar to cellulose whisker, with so many advantages over conventional inorganic nanoparticles such as low density, non-toxicity, biodegradability, biocompatibility and easy surface modification and functionalization, chitin whiskers, within or without modification, are supposed to find extensive application in many areas such as reinforcing nanocomposites, cosmetic, food industry, drug delivery, tissue engineering. However, recent studies have mainly focused on the preparation and applications of nanocomposite based on chitin whiskers; less attention has been paid on other application areas. For the future studies, more attention should be focused on developing novel applications of chitin whiskers. Even for the chitin reinforced nanocomposites, there will still be a lot of valuable works to be done for future research, for example, developing new simple and effective processing methods so as to commercialize high performance polymer/chitin whisker composites, producing polymer nanocomposites filled with individual chitin whiskers which would create much more reinforcing efficiency than the conventional chitin whisker due to the high aspect ratio of individual chitin whisker. Then, great endeavors are necessary to make this area more prosperous and fruitful. In a word, there are abundant of opportunities combined with challenges in chitin whisker related scientific and industrial fields.

## References

1. Richard, A.G.: The Integument of Arthropods. University of Minnesota Press, Minneapolis (1951)
2. Rudall, K.M.: Conformation of chitin-protein complexes. In: Ramachandran, G.N. (ed.) Conformation of Biopolymers. Academic, London (1967)
3. Weis-Fogh, T.: Structure and formation of insect cuticle. Symposia R. Entomolo. Soc. **5**, 165–183 (1970)
4. Kumar, M.N.V.R.: A review of chitin and chitosan application. React. Funct. Polym. **46**, 1–27 (2000)
5. Kobayashi, S., Kiyosada, T.: Shoda, S.-i.: Synthesis of artificial chitin: irreversible catalytic behavior of glycosyl hydrolase through a transition state analogue substrate. J. Am. Chem. Soc. **118**, 13113–13114 (1996)

6. Sakamoto, J., Sugiyama, J., Kimura, S., Imai, T., Itoh, T., Watanabe, T., Kobayashi, S.: Artificial Chitin Spherulites Composed of Single Crystalline Ribbons of alpha-Chitin via Enzymatic Polymerization. Macromolecules. **33**, 4155–4160 (2000)
7. Kadokawa J.-i.: Precision polysaccharide synthesis catalyzed by enzymes. Chem. Rev. 111, 4308–4345 (2011)
8. Ravikumar, M.N.V.B.: Chitin and chitosan fibres: a review. Mater. Sci.C. 22, 905–915 (1999)
9. Rinaudo, M.: Chitin and chitosan: Properties and applications. Prog. Polym. Sci. **31**, 603–632 (2006a)
10. Pillai, C.K.S., Paul, W., Sharma, C.P.: Chitin and chitosan polymers: Chemistry, solubility and fiber formation. Prog. Polym. Sci. **34**, 641–678 (2009)
11. Bordes, P., Pollet, E., Averous, L.: Nano-biocomposites: Biodegradable polyester/nanoclay systems. Prog. Polym. Sci. **34**, 125–155 (2009a)
12. Okada, A., Usuki, A.: Macromolecular Materials and Engineering Twenty Years of Polymer-Clay Nanocomposites. Macromol. Mater. Eng. **291**, 1449–1476 (2006)
13. Usuki, A., Hasegawa, N., Kato, M.: Polymer-clay nanocomposites. Adv. Polym. Sci. **179**, 135–195 (2005)
14. Chen, B.Q., Evans, J.R.G.: Impact strength of polymer-clay nanocomposites. Soft Matter. **5**, 3572–3584 (2009)
15. Le Corre, D., Bras, J., Dufresne, A.: Starch Nanoparticles: A Review. Biomacromolecules. **11**, 1139–1153 (2010)
16. Favier, V., Chanzy, H., Cavaille, J.Y.: Polymer nanocomposites reinforced by cellulose whiskers. Macromolecules. **28**, 6365–6367 (1995)
17. Habibi, Y., Lucia, L.A., Rojas, O.: Cellulose nanocrystals: chemistry, self-assembly, and applications. Chem Review. J. Chem. Rev. **110**, 3479–3500 (2010)
18. Chen, L., Zhu, M.F., Song, L.Y., Yu, H., Zhang, Y., Chen, Y.M., Adler, H.: Crystallization behavior and thermal properties of blends of poly(3-hydroxybutyrateco-3-valerate) and poly(1,2-propandiolcarbonate). J. Macromol. Symp. **210**, 241–250 (2004)
19. Angles, M.N., Dufresne, A.: Plasticized starch/tunicin whiskers nanocomposites. 1. Structural analysis. Macromolecules. **33**, 8344–8353 (2000)
20. Angles, M.N., Dufresne, A.: A. Plasticized starch/tunicin whiskers nanocomposite materials. 2. Mechanical behavior. Macromolecules. **34**, 2921–2931 (2001)
21. Samir, M.A.S.A., Alloin, F., Dufresne, A.: Review of recent research into cellulosic whiskers, their properties and their applications in nanocomposite field. Biomacromolecules. **6**, 612–626 (2005)
22. Siqueira, G., Bras, J., Dufresne, A.: Cellulosic BioNCs: A review of preparation. Properties and applications. Polymers. **2**, 728–765 (2010a)
23. Klemm, D., Kramer, F., Moritz, S., Lindstrom, T., Ankerfors, M., Gray, D., Dorris, A.: "Nanocelluloses: A new family of nature-based materials. Angew. Chem. Int. Ed. **50**, 5438–5466 (2011)
24. Siqueira, G., Bras, J., Dufresne, A.: Cellulose Whiskers versus Microfibrils: Influence of the Nature of the Nanoparticle and its Surface Functionalization on the Thermal and Mechanical Properties of Nanocomposites. Biomacromolecules. **10**, 425–432 (2009)
25. Dufresne, A.: Cellulose Whiskers versus Microfibrils: Influence of the Nature of the Nanoparticle and its Surface Functionalization on the Thermal and Mechanical Properties of Nanocomposites. Can. J. Chem. **86**, 484–494 (2008)
26. Fan, Y., Saito, T., Isogai, A.: Preparation of chitin nanofibers from squid pen beta-chitin by simple mechanical treatment under acid conditions. Biomacromolecules. **9**, 1919–1923 (2008a)
27. Revol, J.-F., Marchessault, R.H.: In vitro nematic ordering of chitin crystallites. Int. J. Biol. Macromol. **15**, 329–335 (1993a)
28. Marchessault, R.H., Morehead, F.F., Walter, N.M.: Liquid crystal systems from fibrillar polysaccharides. Nature. **184**, 632–633 (1959a)

29. Li, J., Revol, J.F., Naranjo, E., Marchessault, R.H.: Effect of electrostatic interaction on phase separation behaviour of chitin crystallite suspensions. Int. J. Biol. Macromol. **18**, 177–187 (1996a)
30. Roberts, G.: Chitin Chemistry. Macmillan, London (1998a)
31. Giraud-Guille, M.M., Belamie, E., Mosser, G.: Organic and mineral network in carapaces, bones and biomimetic materials. Comptes Rendus Palevol. **3**, 503–513 (2004)
32. Marchessault, R.H., Morehead, F.F., Walter, N.M.: Liquid crystal systems from fibrillar polysaccharides. Nature. **184**, 632–633 (1959b)
33. Dufresne, A., Kellerhals, M.B., Witholt, B.: Transcrystallization in mcl-PHAs/ cellulose whiskers composites. Macromolecules. **32**, 7396–7401 (1999)
34. Revol, J.-F., Marchessault, R.H.: In vitro chiral nematic ordering of chitin crystallites. Int. J. Biol. Macromol. **15**, 329–335 (1993b)
35. Li, J., Revol, J.F., Marchessault, R.H.: Rheological properties of aqueous suspensions of chitin crystallites. J. Colloid Interface Sci. **183**, 365–373 (1996b)
36. Paillet, M., Dufresne, A.: Chitin whiskers reinforced thermoplastic nanocomposites. Macromolecules. **34**, 6527–6530 (2001)
37. Morin, A., Dufresne, A.: Nanocomposites of chitin whiskers from Riftia tubes and poly(caprolactone). Macromolecules. **35**, 2190–2199 (2002)
38. Lu, Y.S., Weng, L.H., Zhang, L.N.: Morphology and properties of soy protein isolate thermoplastics reinforced with chitin whiskers. Biomacromolecules. **5**, 1046–1051 (2004)
39. Nair, K.G., Dufresne, A.: "Crab shell chitin whisker reinforced natural rubber nanocomposites. 1. Biomacromolecules. **4**, 657–665 (2003a)
40. Wu, X., Torres, F.G., Vilaseca, F., Peijs, T.: Influence of the processing conditions on the mechanical properties of chitin whisker reinforced poly(caprolactone) nanocomposites. J. Biobased Mater. Bio. **1**, 341–350 (2007)
41. Sriupayo, J., Supaphol, P., Blackwell, J., Rujiravanit, R.: Preparation and characterization of @a-chitin whisker-reinforced chitosan nanocomposite films with or without heat treatment. Carbohydr. Polym. **62**, 130–136 (2005a)
42. Sriupayo, J., Supaphol, P., Blackwell, J., Rujiravanit, R.: Preparation and characterization of α-chitin whisker-reinforced poly(vinyl alcohol) nanocomposite films with or without heat treatment. Polymer. **46**, 5637–5644 (2005b)
43. Goodrich, J.D., Winter, W.T.: α-Chitin Nanocrystals Prepared from shrimp shells and their specific surface area measurement. Biomacromolecules. **8**, 252–257 (2007)
44. Watthanaphanit, A., Supaphol, P., Tamura, H., Tokura, S., Rujiravanit, R.: Fabrication, structure and properties of chitin whisker-reinforced alginate nanocomposite fibers. J. Appl. Polym. Sci. **110**, 890–899 (2008)
45. Clark, G.L., Smith, A.F.: X-ray diffraction studies of chitin, chitosan and derivatives. J. Phys. Chem. **40**, 863–879 (1936a)
46. Montanari, S., Rountani, M., Heux, L., Vignon, M.R.: Topochemistry of carboxylated cellulose nanocrystals resulting from TEMPO-mediated oxidation. Macromolecules. **38**, 1665–1671 (2005)
47. Saito, T., Nishiyama, Y., Putaux, J.L., Vignon, M., Isogai, A.: Natural Polymers: Volume 2: Nanocomposites. Biomacromolecules. **7**, 1687–1691 (2006)
48. Fukuzumi, H., Saito, T., Wata, T., Kumamoto, Y., Isogai, A.: Transparent and high gas barrier films of cellulose nanofibers prepared by TEMPO-mediated oxidation. Biomacromolecules. **10**, 162–165 (2009)
49. Ishii, D., Saito, T., Isogai, A.: Viscoelastic Evaluation of Average Length of Cellulose Nanofibers Prepared by TEMPO-Mediated Oxidation. Biomacromolecules. **12**, 548–550 (2011)
50. Saito, Y., Putaux, J.-L., Okano, T., Gaill, F., Chanzy, H.: Structural aspects of the swelling of chitin in HCl and its conversion into α-chitin. Macromolecules. **30**, 3867–3873 (1997)
51. Fan, Y., Saito, T., Isogai, A.: Chitin nanocrystals prepared by TEMPO-mediated oxidation of alpha-chitin. Biomacromolecules. **9**, 192–198 (2008b)

52. Fan, Y.M., Saito, T., Isogai, A.: Individual chitin nano-whiskers prepared from partially deacetylated α-chitin by fibril surface cationization. Carbohydr. Polym. **79**, 1046–1051 (2010)
53. Hariraksapitak, P., Supaphol, P.: Preparation and properties of a-chitin-whisker-reinforced hyaluronangelatin nanocomposite scaffolds. J. Appl. Polym. Sci. **117**, 3406–3418 (2010)
54. Bustos, R.O., Healy, M.G.: Proceedings Icheme Research Event. London **4–6**, 126–128 (1994)
55. Phongying, S., Aiba, S., Chirachanchai, S.: Direct chitosan nanoscaffold formation via chitin whiskers. Polymer. **48**, 393–400 (2007)
56. Horton, D., Lineback, D.R.: N-deacetylation, chitodan from chitin. In: Whistler, R.L., Wolfson, M.L. (eds.) Methods in Carbohydrate Chemistry, p. 403. Academic, New York (1965)
57. Park, S.-I., Zhao, Y.: Incorporation of a high concentration of mineral or vitamin into chitosan-based films. J. Agric. Food Chem. **52**, 1933–1939 (2004)
58. Domard, A., Rinadudo, M.I.: Preparation and characterization of fully deacetylated chitosan. J. Biol. Macromol. **5**, 49–52 (1983)
59. Pelletier, A., Lemire, I., Sygusch, J., Chornet, E., Overend, R.P.: Chitin/chitosan transformation by thermo-mechano-chemical treatment including characterization by enzymatic depolymerization. Biotechnol. Bioeng. **36**, 310–315 (1990)
60. Focher, B., Beltrane, P.L., Naggi, A., Torri, G.: Alkaline N-deacetylation of chitin enhanced by flash treatments: Reaction kinetics and structure modifications. Carbohydr. Polym. **12**, 405–418 (1990)
61. Goycoolea, F.M., Higuera, C.I., Hernandez, J.L.J., García, K.D.: Advances in Chitin Science. Lyon: Jacques André, pp. 78–83 (1998)
62. Mima, S., Miya, M., Iwamoto, R., Yoshikawa, S.: Microwave technique for efficient deacetylation of chitin nanowhiskers to a chitosan nanoscaffold. J Appl. Polym. Sci. **28**, 1909–1917 (1983)
63. Gooday, G.W., Prosser, J.I., Hillman, K., Cross, M.G.: Functional characterization of chitin and chitosan. Biochem. Syst. Ecol. **19**(5), 395–400 (1991)
64. Lertwattanaseri, T., Ichikawa, N., Mizoguchi, T., Tanaka, Y., Chirachanchai, S.: Natural Chelating Polymers. Carbohydr. Res. **344**, 331–335 (2009a)
65. Aranaz, I., Mengíbar, M., Harris, R., Paños, I., Miralles, B., Acosta, N., Galed, G., Heras, A.: Functional characterization of chitin and chitosan. Curr. Chem. Biol. **3**, 203–230 (2009a)
66. Muzzarelli, R.A.A.: In: Muzzarelli, R.A.A. (ed.) Chitin Handbook, pp. 153–65. Grottamore, European Chitin Society (1977)
67. Choi, W., Ahn, K., Lee, D., Byun, M., Park, H.: Preparation of chitosan oligomers by irradiation. Polym. Degrad. Stabil. **78**, 533–538 (2002)
68. Kassai, M.: A review of several reported procedures to determine the degree of N-acetylation for chitin and chitosan using infrared spectroscopy. Carbohydr. Polym. **71**, 497–508 (2008)
69. Nair, K.G., Dufresne, A.: Crab shell chitin whisker reinforced natural rubber nanocomposites. Biomacromolecules. **4**, 657–665 (2003b)
70. Kvien, I., Bjørn, S.T., Oksman, K.J.: Characterization of cellulose whiskers and their nanocomposites by atomic force and electron microscopy. Biomacromolecules. **6**, 3160–3165 (2005)
71. Gopalan, K.N., Dufresne, A.: Effect of chemical modification of chitin whiskers. J. Biomacromolecules. **4**, 1835–1842 (2003a)
72. Gopalan, N.K., Dufresne, A.: Crab shell chitin whisker reinforced natural rubber nanocomposites. 1. Processing and swelling behavior. J. Biomacromolecules. **4**, 657–665 (2003b)
73. Michel, P., Dufresne, A.: Chitin Whisker Reinforced Thermoplastic Nanocomposites. J. Macromolecules. **34**, 19 (2001)
74. M. Wada., Y. Saito.: J. Polym. Sci. B: Lateral thermal expansion of chitin crystals. Polym. Phys. 39, 168–174 (2001)

75. Feng, F., Liu, Y., Hu, K.: Influence of alkali-freezing treatment on the solid state structure of chitin. Carbohydr. Res. **339**, 2321–2324 (2004)
76. Li, J., Revol, J.F., Marchessault, R.H.: Effect of degree of deacetylation of chitin on the properties of chitin crystallites. J. Appl. Polym. Sci. **65**, 373–380 (1997)
77. Jayakumar, R., Tamura, T.: Synthesis, characterization and thermal properties of chitin-&-poly(€-caprolactone) copolymers by using chitin gel. Int. J. Biol. Macromol. **43**, 32–36 (2008)
78. Mathew, A.P., Laborie, M.P.G., Oksman, K.: Cross-linked chitosan α-chitin whiskers nanocomposites with improved permeation selectivity and pH stability. J. Biomacromolecules. **10**, 1627–1632 (2009)
79. Hein, S., Ng, C. H., Chandrkrachang, S., Stevens, W.F.: A systematic approach to quality assessmentsystem of chitosan. Chitin and Chitosan: Chitin and Chitosan in Life Science. Yamaguchi. 327–335 (2001)
80. ISO 10993-18:200s5 Biological evaluation of medical devices, Part 18: Chemical characterizations of material
81. ISO/DIS 10993-19 Biological evaluation of medical devices, Part 19: Physico-chemical, mechanical and morphological characterization
82. Sriupayo, J., Supaphol, P., Blackwell, J., Rujiravanit, R.J.: Preparation and characterization of α-chitin whisker-reinforced poly(vinyl alcohol) nanocomposite films with or without heat treatment. Polymer. **46**, 5637–5644 (2005c)
83. Angellier, H., Boisseau, S.M., Lebrun, L., Dufresne, A.: Processing and structural properties of waxy maize starch nanocrystals reinforced natural rubber. J. Macromolecules. **38**, 3783–3792 (2005a)
84. Alonso, B., Belamie, E.: Chitin–Silica Nanocomposites by Self-Assembly. Angewandte. Chemie. **122**(44), 8377–8380 (2010)
85. Feng, L., Zhou, Z., Dufresne, L., Huang, J., Wei, M., An, L.J.: Structure and Properties of New Thermoforming Bionanocomposites Based on Chitin Whisker-Graft-Polycaprolactone. Appl. Polym. Sci. **112**, 2830–2837 (2009a)
86. Van de Velde, K., Kiekens, P.: Structure analysis and degree of substitution of chitin, chitosan and dibutyrylchitin by FT-IR spectroscopy and solid state $^{13}C$ NMR. Carbohydr. Polym. **58**, 409–416 (2004)
87. Varum, K.M., Antohonsen, M.W., Grasdalen, H., Smidsrod, O.: Determination Of The Degree Of N-Acetylation And The Distributionof N-Acetyl Groups In Partially N-Deacetylated Chitins (Chitosans)By High-Field NMR-Spectroscopy. Carbohyd. Res. **211**, 17–23 (1991)
88. Ramaprasad, T., Rao, V., Sanjeev, G.: Synthesis of chitin-polyaniline nanocomposite by electron beam irradiation. J. Appl. Polym. Sci. **121**, 623–633 (2011)
89. Ruiz-Hitzky, E., Darder, M.: Special Issue on trends in Biohybrid Nanostructured Materials. Curr. Nanosci. **2**, 153–294 (2006)
90. Pandey, J.K., Kumar, A.P., Misra, M., Mohanty, A.K., Drzal, L.T., Singh, R.P.: Recent advances in biodegradable nanocomposites. J. Nanosci. Nanotech. **5**, 497–526 (2005)
91. Ikoma, T., Muneta, T., Tanaka, J.: Key Engineering Materials. Key Eng. Mater. **192–1**, 487–490 (2000)
92. Kikuchi, M., Itoh, S., Ichinose, S., Shinomiya, K., Tanaka, J.: Self-Organization Mechanism in a Bone-like Hydroxyapatite/Collagen Nanocomposite Synthesized in vitro and Its Biological Reaction in vivo. Biomaterials. **22**, 1705–1711 (2001)
93. Wang, K.: In: Yin Y CRC Press, pp. 339–406, ISBN: 978-1-4398-2114-5
94. Zia, K.M., Barikani, M., Zuber, M., Bhatti, I.A., Sheikh, M.A.: Molecular engineering of chitin based polyurethane elastomers. Carbohydr. Polym. **74**, 149–158 (2008a)
95. Zia, K.M., Barikani, M., Bhatti, I.A., Zuber, M., Bhatti, H.N.: Synthesis and characterization of novel biodegradable thermally stable chitin based polyurethane elastomers. J. App. Polym. Sci. **110**, 769–776 (2008b)

96. Zia, K.M., Zuber, M., Bhatti, I.A., Barikani, M., Sheikh, M.A.: Evaluation of biocompatibility and mechanical behavior of polyurethane elastomers based on chitin/1,4-butane diol blends. Int. J. Biolog. Macromol. **44**, 18–22 (2009a)
97. Zia, K.M., Zuber, M., Bhatti, I.A., Barikani, M., Sheikh, M.A.: Evaluation of biocompatibility and mechanical behavior of chitin polyurethane elastomers, Part-II: Effect of diisocyanate structure. Int. J. Biol. Macromol. **44**, 23–28 (2009b)
98. Barikani, M., Zia, K.M., Bhatti, I.A., Zuber, M., Bhatti, H.N.: Molecular engineering and properties of chitin based shape memory polyurethane elastomers. Carbohydr. Polym. **74**(3), 621–626 (2008)
99. Zia, K.M., Zuber, M., Barikani, M., Bhatti, I.A., Khan, M.B.: Surface characteristics of chitin based shape memory polyurethane elastomers. Colloids Surf. B. **72**, 248–252 (2009c)
100. Kaczmarek, H., Chaberska, H.: The influence of UV-irradiation and support type on surface properties of poly(methyl methacrylate) thin films, Journal of Photochemistry and Photobiology. App. Surf. Sci. **252**, 8185–8192 (2006)
101. Kaczmarek, H., Podgorski, A.: J. Photochem. Photobiol. A: The effect of UV-irradiation on poly(vinyl alcohol) composites with montmorillonite. Journal of Photochemistry and Photobiology. Journal of Photochemistry and Photobiology. Chemi. **191**, 209–215 (2007)
102. Zia, K.M., Bhatti, H.N., Bhatti, I.A.: Methods for polyurethane and polyurethane composites, recycling and recovery. Funct. Polym. 67, 675–692
103. Zia, K.M., Barikani, M., Zuber, M., Bhatti, I.A.: Surface Characteristics of UV-irradiated Polyurethane Elastomers extended with alkane Diols Islam-ud-Din. App. Surf. Sci. **254**, 6754–6761 (2008c)
104. Matsushita, Y., Suzuki, A., Sekiguchi, T., Saito, K., Imai, T., Fukushima, K.: Mapping of the cationic Starch adsorbed on pulp fibers by tof-SIMS App. Surf. Sci. **255**, 1022–1024 (2008)
105. Yokota, S., Kitaoka, T., Wariishi, H.: Surface morphology of cellulose films prepared by spin coating on silicon oxide substrates pretreated with cationic polyelectrolyte. App. Surf. Sci. **253**, 4208–4214 (2008)
106. Santosa, S.J., Siswanta, D., Sudiono, S., Utarianingrum, R.: Chitin–humic acid hybrid as adsorbent for Cr(III) in effluent of tannery wastewater treatment. Journal of Photochemistry and Photobiology. App. Surf. Sci. **254**, 7846–7850 (2008)
107. Zia, K.M., Barikani, M., Khalid, A.M., Honarkar, H.: Surface characteristics of polyurethane elastomers based on chitin/1,4-butanediol blends. Ehsan-ulHaq. Carbohydr. Polym. **77**, 621–627 (2009d)
108. Zia, K.M., Barikani, M., Zuber, M., Bhatti, I.A., Barmar, M.: Surface characteristics of polyurethane elastomers based on chitin/1,4-butanediol blends. Int. J. Biol. Macromol. **44**, 182–185 (2009e)
109. Zia, K.M., Barikani, M., Zuber, M., Bhatti, I.A., Barmar, M.: "XRD studies of UV irradiated chitin-based polyurethane elastomers. Carbohydr. Polym. **77**, 54–58 (2009f)
110. Zia, K.M., Bhatti, I.A., Barikani, M., Zuber, M., Bhatti, H.N.: XRD studies of polyurethane elastomers based on chitin/1,4-butane diol blends. Carbohydr. Polym. **76**, 183–187 (2009g)
111. Nishio, Y., Koide, T., Miyashita, Y., Kimura, N., Suzuki, H.J.: Water-Soluble Polymer Blends with Partially Deacetylated Chitin: A Miscibility Characterization. Appl. Polym. Sci. **37**, 1533–1538 (1999)
112. Kim, J.Y., Ha, C.S., Jo, N.J.: Synthesis and properties of biodegradable chitin-*graft*-poly(L-lactide) copolymers Polym. Int. **51**, 1123–1128 (2002)
113. Zuber, M., Zia, K.M., Mahboob, S., Hassan, M., Bhatti, I.A.: Synthesis of chitin-bentonite clay based polyurethane bio-nanocomposites Int. J. Biol. Macromol. **47**, 196–200 (2010)
114. Cardenas, G., Cabrera, G., Taboada, E., Miranda, S.P.: Chitin characterization by SEM, FTIR, XRD, and 13C cross polarization/mass angle spinning NMR. J. Appl. Polym. Sci. **93**, 1876–1885 (2004)
115. Wang, S.F., Shen, L., Tong, Y.J., Chen, L., Phang, I.Y., Lim, P.Q., Liu, T.X.: Biopolymer Chitosan/Montmorillonite Nanocomposites: Preparation and Characterization. Polym. Degrad. Stab. **90**, 123 (2005)

116. Darder, M., Colilla, M., Ruiz-Hitzky, E.: Biopolymer-clay Nanocomposites based on chitosan intercalated in montmorillonite. NMR. Chem. Mater. **15**, 3774–3780 (2003a)
117. Darder, M., Lopez-Blanco, M., Aranda, P., Leroux, F., Ruiz-Hitzky, E.: Bionanocomposites Based on layered double hydroxides. Chem. Mater. **17**, 1969–1977 (2005)
118. Darder, M., Lopez-Blanco, M., Aranda, P., Aznar, A.J., Bravo, J., Ruiz-Hitzky, E.: Microfi brous chitosan-sepiolite nanocomposites. Chem. Mater. **18**, 1602–1610 (2006)
119. Darder, M., Colilla, M., Ruiz-Hitzky, E.: Biopolymer-clay nanocomposites based on Chitosan intercalated in montmorillonite. Chem. Mater. **15**(20), 3774–3780 (2003b)
120. Xin, Y., Guanghan, L., Xiaogang, W., Tong, Z.: Studies on Electrochemical Behavior of Bromideat a Chitosan-Modified Glassy Carbon Electrode. Electroanalysis. **13**, 923–926 (2001)
121. Lu, G., Yao, X., Wu, X., Zhan, T.: Determination of the total iron by chitosan-modified Glassy carbon electrode. Microchem. J. **69**, 81–87 (2001)
122. Zhao, C.-Z., Egashira, N., Kurauchi, Y., Ohga, K.: Electrochemiluminescence sensor having a pt electrode coated with a ru(bpy)(3)(2-modified chitosan silica-gel membrane. Anal. Sci. **14**, 439–441 (1998)
123. Khan, T.A., Peh, K.K.: Ch'ng, H.S.: Reporting degree of deacetyla-tion values of chitosan: The influence analytical methods. J. Pharm. Pharm. Sci. **5**, 205–212 (2002)
124. Giles, C.H., MacEwan, T.H., Nakhwa, S.N., Smith, D.J.: A system of classification of solution adsorption isotherms and its use in diagnosis of adsorption mechanisms and in measurements of specific Areas of soils. Chem. Soc. 3973–3993 (1960)
125. Miller, R., Fainerman, V.B.: Möhwald, H.: Adsorption behaviour of oxyethylated surfactants at the air/water interface. J. Colloid Interface Sci. **247**, 193–199 (2002)
126. Huang, H., Yuan, Q., Yang, X.: Preparation and characterization of metal-chitosan nanocomposites. Colloid Surf.B. 39(1–2):31–37
127. Clark, G.L., Smith, A.F.: X Ray diffraction studies of Chitin. Chitosan and Derivatives. J. Phys. Chem. **40**, 863–879 (1936b)
128. Van Olphen, H.: Preparation and characterization of metal-chitosan nanocomposites. An introduction to clay colloid chemistry, 2nd edn. Wiley-Interscience, New York (1977)
129. Aranaz, I., Mengíbar, M., Harris, R., Paños, I., Miralles, B., Acosta, N., Galed, G., Heras, A.: Functional characterization of chitin and chitosan. Curr. Chem. Biol. **3**, 203–230 (2009b)
130. Ray, S.S., Yamada, K., Okamoto, M., Ueda, K.: New polylactide-layered silicate nanocomposites. 2. Concurrent Improvements of material properties, biodegradability and melt rheology. Polymer. **44**, 857–866 (2003)
131. Alexandre, M., Dubois, P. Mater. Polymer-layered silicate nanocomposites: Preparation, properties and uses of a new class of materials. Sci. Eng. R: Rep. 28, 1–63 (2000)
132. Pavlidoua, S., Papaspyrides, C.D.: A review on polymer–layered silicate nanocomposites. Prog. Polym. Sci. **33**, 1119–1198 (2008)
133. Bordes, P., Pollet, E., Averous, L.: Nano-biocomposites: Biodegradable polyester/nanoclay systems. Prog. Polym. Sci. **34**, 125–155 (2009b)
134. Dufresne, A., Cavaille, J.Y., Helbert, W.: New nanocomposite materials: microcrystalline starch reinforced thermoplastic. Macromolecules. **29**, 7624–7626 (1996)
135. Dubief, D., Samain, E., Dufresne, A.: Polysaccharide microcrystals reinforced amorphous poly($\beta$-hydroxyoctanoate) nanocomposite materials. Macromolecules. **32**, 5765–5771 (1999a)
136. Grunert, M., Winter, W.T.: Nanocomposites of cellulose acetate butyrate reinforced with cellulose nanocrystals. J. Polym. Environ. **10**, 27–30 (2002)
137. Samir, M.A.S.A., Alloin, F., Paillet, M., Dufresne, A.: Tangling effect in fibrillated cellulose reinforced nanocomposite. Macromolecules. **37**, 4313–4316 (2004a)
138. Samir, M.A.S.A., Alloin, F., Sanchez, J.Y., El Kissi, N., Dufresne, A.: Preparation of cellulose whiskers reinforced nanocomposites from an organic medium suspension. Macromolecules. **37**, 1386–1393 (2004b)

139. Nair, K.G., Dufresne, A.: Crab Shell Chitin Whisker Reinforced Natural Rubber Nanocomposites. 2. Mechanical Behavior. Biomacromolecules. **4**, 666–674 (2003c)
140. Nair, K.G., Dufresne, A., Gandini, A., Belgacem, M.N.: Crab shell chitin whiskers reinforced natural rubber nanocomposites. 3. Effect of chemical modification of chitin whiskers. Biomacromolecules. **4**, 1835–1842 (2003)
141. Li, Q., Zhou, J.P., Zhang, L.N.: J. Polym. Sci.Part B: Starch-based composites reinforced with novel chitin nanoparticles. Polym. Phys. 47, 1069–1077 (2009)
142. Chang, P.R., Jian, R.J., Yu, J.G., Ma, X.F.: Chitin whiskers: an overview. Carbohydr. Polym. 80, 420–425, (4123–4135) (2010)
143. Zeng, J-B., He, Y-S., Li, S-L., Wang, Y-Z.: Biomacromolecules. dx.doi.org/10.1021/bm201564a (2012)
144. Huang, J., Zou, J.W., Chang, P.R., Yu, J.H., Dufresne, A.: New waterborne polyurethane-based nanocomposites reinforced with low loading levels of chitin whisker. Express Polym. Lett. **5**, 362–373 (2011)
145. Feng, L.D., Zhou, Z.Y., Dufresne, A., Huang, J., Wei, M., An, L.J.: Structure and properties of new thermoforming bionanocomposites based on chitin whisker-graft-polycaprolactone. J. Appl. Polym. Sci. **112**, 2830–2837 (2009b)
146. Yuan, H.H., Nishiyama, Y., Wada, M., Kuga, S.: Surface acylation of whiskers by drying aqueous emulsion. Biomacromolecules. **7**, 696–700 (2006)
147. Siqueira, G., Bras, J., Dufresne, A.: New process of chemical grafting of cellulose nanoparticles with a long chain isocyanate. Langmuir. **26**, 402–411 (2010b)
148. Gousse, C., Chanzy, H., Excoffier, G., Soubeyrand, L., Fleury, E.: Stable suspensions of partially silylated cellulose whiskers dispersed in organic solvents. Polymer. **43**, 2645–2651 (2002)
149. Oksman, K., Mathew, A.P., Bondeson, D., Kvien, I.: Manufacturing process of cellulose whiskers/polylactic acid nanocomposites. Compos. Sci. Technol. **66**, 2776–2784 (2006)
150. Bondenson, D., Oksman, K.: Polylactic acid/cellulose whisker nanocomposites modified by polyvinyl alcohol. Compos. Part A. **38**, 2486–2492 (2007)
151. de Menezes, A.J., Siqueira, G., Curvelo, A.A.S.: Extrusion and characterization of functionalized cellulose whisker reinforced polyethylene Nanocomposites. Polymer. **50**, 4552–4563 (2009)
152. Pan, J.R., Huang, C., Chen, S., Chung, Y.-C.: Evaluation of a modified chitosan biopolymer for coagulation of colloidal particles. Colloids Surf. A. **147**, 359–364 (1999)
153. Nakagaito, A.N., Yano, H.: The effect of morphological changes from pulp fiber towards nano-scale fibrillated cellulose on the mechanical properties of high-strength plant fiber based composites. Appl. Phys. A. **78**, 547–552 (2004)
154. Nakagaito, A.N., Iwamoto, S., Yano, H.: Bacterial cellulose: the ultimate nano-scalar cellulose morphology for the production of high-strength composites. Appl. Phys. A. **80**, 93–97 (2005)
155. Shimazaki, Y., Miyazaki, Y., Takezawa, Y., Nogi, M., Abe, K., Ifuku, S., Yano, H.: Excellent thermal conductivity of transparent cellulose nanofiber/epoxy resin nanocomposites. Biomacromolecules. **8**, 2976–2978 (2007)
156. Nogi, M., Handa, K., Nakagaito, A.N., Yano, H.: Optically transparent bionanofiber composites with low sensitivity to refractive index of the polymer matrix. Appl. Phys. Lett. **87**, 243110–243112 (2005)
157. Iwamoto, S., Abe, K., Yano, H.: The effect of hemicelluloses on wood pulp nanofibrillation and nanofiber network characteristics. Biomacromolecules. **9**, 1022–1026 (2008)
158. Henriksson, M., Berglund, L.A.: Structure and properties of cellulose nanocomposite films containing melamine formaldehyde. J. Appl. Polym. Sci. **106**, 2817–2824 (2007)
159. Seydibeyoğlu, M.Ö., Oksman, K.: Novel nanocomposites based on polyurethane and micro fibrillated cellulose. Compos. Sci. Technol. **68**, 908–914 (2008)
160. Eyholzer, Ch., Bordeanu, N., Lopez-Suevos, F., Rentsch, D., Zimmermann, T., Oksman, K.: Preparation and characterization of water-redispersible nanofibrillated cellulose in powder form. Cellulose. **17**, 19–30 (2010)

161. Park, I., Kang, M., Kim, H.S., Jin, H.J.: Electrospinning of poly(ethylene oxide) with bacterial cellulose whiskers. Macromol. Symp. **249–250**, 289–294 (2007)
162. Rojas, O.J., Montero, G.A., Habibi, Y.: Electrospun nanocomposites from polystyrene loaded with cellulose nanowhiskers. J. Appl. Polym. Sci. **113**, 927–935 (2009)
163. Zoppe, J.O., Peresin, M.S., Habibi, Y., Venditti, R.A., Rojas, O.J.: Reinforcing poly(-caprolactone) nanofibers with cellulose nanocrystals. ACS Appl. Mater. Interfaces. **1**, 1996–2004 (2009)
164. Peresin, M.S.: Habibi, Y, Zoppe, J.O., Pawlak, J.J., Rojas, O.J.: Nanofiber composites of polyvinyl alcohol and cellulose nanocrystals: manufacture and characterization. Biomacromolecules. **11**, 674–681 (2010)
165. de Mesquita, J.P., Donnici, C.L., Pereira, F.V.: Biobased nanocomposites from layer-by-layer assembly of cellulose nanowhiskers with chitosan. Biomacromolecules. **11**, 473–480 (2010)
166. Podsiadlo, P., Choi, S.Y., Shim, B., Lee, J., Cuddihy, M., Kotov, N.A.: Molecularly engineered nanocomposites: layer-by-layer assembly of cellulose nanocrystals. Biomacromolecules. **6**, 2914–2918 (2005)
167. Cranston, E.D., Gray, D.G.: Formation of cellulose-based electrostatic layer-by-layer films in a magnetic field. Sci. Technol. Adv. Mater. **7**, 319–321 (2006a)
168. Cranston, E.D., Gray, D.G.: Morphological and optical characterization of polyelectrolyte multilayers incorporating nanocrystalline cellulose. Biomacromolecules. **7**, 2522–2530 (2006b)
169. Jean, B., Dubreuil, F., Heux, L., Cousin, F.: Structural details of cellulose nanocrystals/polyelectrolytes multilayers probed by neutron reflectivity and AFM. Langmuir. **24**, 3452–3458 (2008)
170. Jean, B., Heux, L., Dubreuil, F., Chambat, G., Cousin, F.: Non-electrostatic building of biomimetic cellulose-xyloglucan multilayers. Langmuir. **25**, 3920–3923 (2009)
171. Aulin, C., Johansson, E., Wågberg, L., Lindström, T.: Self-organized films from cellulose I nanofibrils using the layer-by-layer technique. Biomacromolecules. **11**, 872–882 (2010)
172. Qiu, J.-D., Xie, H.-Y., Liang, R.-P.: Preparation of porous chitosan/carbon modified electrode for biosensor application. Microchim. Acta. **162**, 57–64 (2008)
173. Feng, L., Zhou, Z., Dufresne, A., Huang, J., Wei, M., An, L.: Structure and properties of new thermoforming bionanocomposites based on chitin whisker-graft-polycaprolactone. J. Appl. Polym. Sci. **112**, 2830–2837 (2009c)
174. Brenner, S.S.: Tensile strength of whiskers. J. App. Phys. **27**, 1484 (1956)
175. Dubief, D., Samain, E., Dufresne, A.: Polysaccharide microcrystals reinforced amorphous poly($\beta$-hydroxyoctanoate) nanocomposite materials. Macromolecules. **32**, 5765–5771 (1999b)
176. Paul, D.R., Robeson, L.M.: Polymer nanotechnology: nanocomposites. Polymer. **49**, 3187–3204 (2008)
177. Kristo, E., Biliaderis, C.G.: Physical properties of starch nanocrystal-reinforced pullulan films. Carbohydr. Polym. **68**, 146–158 (2007)
178. Angellier, H., Molina-Boisseau, S., Lebrun, L., Dufresne, A.: Processing and structural properties of waxy maize starch nanocrystals reinforced natural rubber. Macromolecules. **38**, 3783–3792 (2005b)
179. Paralikara, S.A., Simonsen, J., Lombardi, J.: Physical properties of starch nanocrystal-reinforced pullulan films. J. Membr. Sci. **320**, 248–258 (2008)
180. Yu, J., Yang, J., Liu, B., Ma, X.: Preparation and characterization of glycerol plasticized-pea starch/ZnO-carboxymethylcellulose sodium nanocomposites. Bioresour. Technol. **100**, 2832–2841 (2009)
181. Zhang, X.L., Huang, J., Chang, P.R., Li, J.L., Chen, Y.M., Wang, D.X., Yu, J.H., Chen, J.H.: Structure and properties of polysaccharide nanocrystal-doped supramolecular hydrogels based on Cyclodextrin inclusion. Polymer. **51**, 4398–4407 (2010)

182. Wang, X., Ma, J., Wang, Y., He, B.: Structural characterization of phosphorylated chitosan and their applications as effective additives of calcium phosphate cements. Biomaterials. **22**, 2247–2255 (2001)
183. Hirano, S., Noishiki, Y.: The blood compatibility of chitosan and N-acylchitosans. J. Biomed. Mater. Res. **19**, 413–417 (1985)
184. Kuen, Y.L., Wan, S.H.: Won, H.P.:Blood compatibility and biodegradability of partially N-acylated chitosan derivatives. Biomaterials. **16**, 1211–1216 (1995)
185. Hirano, S., Midorikawa, T.: Novel method for the preparation of N-acylchitosan fiber and N-acylchitosancellulose fiber. Biomaterials. **19**, 293–297 (1998)
186. Ono, K., Saito, Y., Yura, H., Ishikawa, K., Kurita, A., Akaike, T., Ishihara, M.: Photocrosslinkable chitosan as a biological adhesive. J. Biomed. Mater. Res. **49**, 289–295 (2000)
187. Khor, E.: Chitin: a biomaterial in waiting. Mater. Sci. **6**, 313–317 (2002)
188. Tomihata, K., Ikada, Y.: In vitro and in vivo degradation of films of chitin and its deacetylated derivatives. Biomaterials. **18**, 567–575 (1997)
189. Onishi, H., Machida, Y.: Biodegradation and Distribution of Water-soluble Chitosan in Mice. Biomaterials. **20**, 175–182 (1999)
190. Tanaka, Y., Tanioka, S.-I., Tanaka, M., Tanigawa, T., Kitamura, Y., Minami, S., Okamoto, Y., Miyashita, M., Nanno, M.: Effects of chitin and chitosan particles on BALB/c mice by oral and parenteral administration. Biomaterials. **18**, 591–595 (1997)
191. Mori, T., Okumura, M., Matsuura, M., Ueno, K., Tokura, S., Okamoto, Y., Minami, S., Fujinaga, T.: Effects of chitin and its derivatives on proliferation and cytokine production of fibroblasts in vitro. Biomaterials. **18**, 947–951 (1997)
192. Prasitsilp, M., Jenwithisuk, R., Kongsuwan, K., Damrongchai, N., Watts, P.: Cellular responses to chitosan in vitro: The importance of deacetylation. J. Mater. Sci. Mater. Med. **11**, 773–778 (2000)
193. Ueno, H., Murakami, M., Okumura, M., Kadosawa, T., Uede, T., Fujinaga, T.: Chitosan accelerates the production of osteopontin from polymorphonuclear leukocytes. Biomaterials. **22**, 1667–1673 (2001)
194. Okamoto, Y., Watanabe, M., Miyatake, K., Morimoto, M., Shigemasa, Y., Minami, S.: Effects of chitin/chitosan and their oligomers/monomers on migration of fibroblasts and vascular endothelium. Biomaterials. **23**, 1975–1979 (2002)
195. Usami, Y., Okamoto, Y., Takayama, T., Shigemasa, Y., Minami, S.: Chitin and chitosan stimulate caine polymorphonclear cells to release leukotrien B4 and prostaglandin E2. J. Biomed. Mater. Res. **42**, 517–522 (1998)
196. Lim, L.Y., Khor, E., Ling, C.E.: Effects of dry heat and saturated steam on the physical properties of chitosan. J. Biomed. Mater. Res. **48**, 111–116 (1999)
197. Lim, L.Y., Khor, E.: Permeability and tensile strength of heated chitosan films. Proceedings of Conference on Challenges for Drug Delivery and Pharmaceutical Technology. p. 196, June 9–11, Tokyo, Japan (1998)
198. Lim, L.Y., Khor, E., Koo, O.: Effects of dry heat and saturated steam on the physical properties of chitosan. J. Biomed. Mater. Res. **43**, 282–290 (1998)
199. Rao, S.B., Sharma, C.P.: Use of chitosan as a biomaterial: studies on its safety and hemostatic potential. J. Biomed. Mater. Res. **34**, 21–28 (1997)
200. Kam, H.M., Khor, E., Lim, L.Y.: Storage of partially deacetylated chitosan films. J. Biomed. Mater. Res. B: Appl. Biomater. **48**, 881–888 (1999)
201. Phongying, S., Aiba, S.I., Chirachanchai, S.: A novel soft and cotton-like chitosan-sugar nanoscaffold. Biopolymers. **83**, 280–288 (2006)
202. Wongpanit, P., Sanchavanakit, N., Pavasant, P., Bunaprasert, T., Tabata, Y., Rujiravanit, R.: Characterization of Chitin Whisker-Reinforced Silk Fibroin Nanocomposite Sponges Eur. Polym. J. **43**, 4123–4135 (2007)
203. Lertwattanaseri, T., Ichikawa, N., Mizoguchi, T., Tanaka, Y., Chirachanchai, S.: Microwave technique for efficient deacetylation of chitin nanowhisker to a chitosan nanoscaffold. Carbohydr. Res. **344**, 331–335 (2009b)

204. Noh, H.K., Lee, S.W., Kim, J.M., Oh, J.E., Kim, K.H., Chung, C.P., Choi, S.C., Park, W.H., Min, B.M.: Electrospinning of chitin nanofibers: degradation behavior and cellular response to normal human keratinocytes and fibroblasts. Biomaterials. **27**, 3934–3944 (2006)
205. Park, K.E., Jung, S.Y., Lee, S.J., Min, B.M., Park, W.H.: Biomimetic nanofibrous scaffolds: preparation and characterization of chitin/silk fibroin blend nanofibers. Int. J. Biolog. Macromol. **38**, 165–173 (2006a)
206. Park, K.E., Kang, H.K., Lee, S.J., Min, B.M., Park, W.H.: Biomimetic nanofibrous scaffolds: Preparation and characterization of PGA/chitin blend nanofibers. Biomacromolecules. **7**, 635–643 (2006b)
207. Shalumon, K.T., Binulal, N.S., Selvamurugan, N., Nair, S.V., Menon, D., Furuike, T., Tamura, H., Jayakumar, R.: Electrospinning of carboxymethyl chitin/poly(vinyl alcohol) nanofibrous scaffolds for tissue engineering applications. Carbohydr. Polym. **77**, 863–869 (2009)
208. Bhattarai, N., Edmondson, D., Veiseh, O., Matsen, F.A., Zhang, M.: Electrospun chitosan-based nanofibers *and* their cellular compatibility. Biomaterials. **26**, 6176–6184 (2005)
209. Subramaniyan, A., Vu, D., Larsen, G.F., Lin, H.Y.: Preparation and evaluation of the electrospun chitosan/PEO fibers for potential applications in cartilage tissue engineering. J. Biomat. Sci.: Polymer Edition. 7, 861–873 (2005)
210. Mo, X., Chen, Z., Weber, H.: Electrospun nanofibers of collagen-chitosan and P(LLA-CL) for tissue engineering. J. Frontier in Material Science. **1**, 20–23 (2007)
211. Zhang, Y.Z., Venugopal, J.R., El-Turki, A., Ramakrishna, S., Su, B., Lim, C.T.: Electrospun biomimetic nanocomposite nanofibers of hydroxyapatite/chitosan for bone tissue engineering. Biomaterials. **29**, 4314–4322 (2008)
212. Yang, D., Jin, Y., Zhou, Y., Ma, G., Chen, X., Lu, F., Nie, J.: In situ mineralization of hydroxyapatite on electrospun chitosan-based nanofibrous scaffolds. Macromol. Biosci. **8**, 239–246 (2008)
213. Zhou, Y.S., Yang, D., Chen, X., Xu, Q., Lu, F., Nie, J.: Electrospun water-soluble carboxyethylchitosan/poly(vinyl alcohol) nano-fibrous membrane as potential wound dressing for skin regeneration. Biomacromolecules. **9**, 349–354 (2008)
214. Feng, Zhang-Qi, Chu, Xuehui, Huang, Ning-Ping, Wang, Tao, Wang, Yichun, Shi, Xiaolei, Ding, Yitao: Zhong-Ze Gu.: The effect of nanofibrous galactosylated chitosan scaffolds on the formation of rat primary hepatocyte aggregates and the maintenance of liver function. Biomaterials. **30**, 2753–2763 (2009d)
215. Rinaudo, M.: Chitin and chitosan: Properties and applications Prog. Polym. Sci. **31**, 603–632 (2006b)
216. Yen, M., Yang, J., Mau, J.: Physicochemical characterization of chitin and chitosan from crab shells Carbohydr. Polym. **75**, 15–21 (2009)
217. Junkasem, J., Rujiravanit, R., Supaphol, P.: Fabrication of a-chitin whisker-reinforced poly(vinyl alcohol) nanocomposite nanofibres by electrospinning. Nanotechnology. **17**, 4519–4528 (2006)
218. Brugnerotto, J., Lizardi, J., Goycoolea, F.M., Arguelles-Monal, W., Desbrieres, J., Rinaudo, M.: An infrared investigation in relation *with* chitin and chitosan characterization. Polymer. **42**(8), 3569–3580 (2001a)
219. Muzzarelli, R.A.A., Rocchetti, R.: Determination of the degree of acetylation of chitosans by first derivative ultraviolet spectrophotometry. Carbohydr. Polym. **6**, 61–72 (1985)
220. Wu, T., Zivanovic, S.: Determination of the degree of acetylation (DA) of chitin and chitosan by an improved first derivative UV method. Carbohyd. Polym. **73**, 248–253 (2008)
221. Duarte, M.L., Ferreira, M.C., Marvao, M.R.: Determination of the degree of acetylation of chitin materials by 13C CP/MAS NMR spectroscopy. I J Biol. Macromol. **28**(5), 359–363 (2001)
222. Raymond, L.: Morin. F.G., Marchessault, R.H.: Degree of deacetylation of chitosan using conductometric titration and solid-state NMR. Carbohydr. Res. **246**(1), 331–336 (1993)
223. Jiang, X., Chen, L., Zhong, W.: A new linear potentiometric titration method for the determination of deacetylation degree of chitosan. Carbohydr. Polym. **54**, 457–463 (2003)

224. Guinesi, L., Cavalheiro, E.: The use of DSC curves to determine the acetylation degree of chitin/chitosan samples. Termochim. Acta. **444**, 128–133 (2006)
225. Rinaudo, M., Milas, M., Le Dung, P.: Characterization of chitosan. Influence of ionic stregth and degree of acetylation on chain expansion. I. J. Biol.Macromol. 15, 281–285 (1993)
226. Brugnerotto, J., Desbrieres, J., Roberts, G., Rinaudo, M.: Characterization of chitosan by steric exclusion chromatography. Polymer. **42**(25), 9921–9927 (2001b)
227. Terbojevich, M.: Cosani, A. In: Muzzarelli, R.A.A., Peter, M.G. (eds.) Chitin Handbook, pp. 87–101. European Chitin Society, Grotammare (1997)
228. ASTM. F2103-01 Standard guide for characterization and testing of chitosan salts as starting materials intended for use in biomedical and tissue-engineered medical product applications (2001)
229. Zia, K.M., Bhatti, I.A., Barikani, M., Zuber, M., Sheikh, M.A. Int. XRD studies of chitin-based polyurethane elastomers. J. Biol. Macromol. 43, 136–141 (2008)
230. Bradford, M.: A rapid and sensitive method for the quantitation of microgram quantities of protein utilizing the principle of protein dye binding. Anal. Biochem. **72**, 248–254 (1976)
231. Roberts, G.: Chitin Chemistry. Macmillan, London (1998b)